Neuronal specific and non-specific responses to cadmium possibly involved in neurodegeneration: a toxicogenomics study in a human neuronal cell model

Forcella M[1]*, Lau P[2]*, Oldani M[1], Melchioretto P[3], Bogni A[2], Gribaldo L[2], Fusi P[1&#] and Urani C[3&#]

[1] Department of Biological Sciences and Biotechnology, University of Milan Bicocca (UniMIB), Piazza della Scienza 2 20126 Milan, Italy

[2]European Commission, DG Joint Research Centre, Via Fermi 2749,21027 Ispra, VA, Italy

[3]Department of Earth and Environmental Sciences, University of Milan Bicocca (UniMIB), Piazza della Scienza 1 20126 Milan, Italy and Mistral University Research Center

[&] Integrated Models for Prevention and Protection in Environmental and Occupational Health, (MISTRAL) University Research Center

*Forcella Matilde and *Lau Pierre contributed equally and are co-first authors

[#] Fusi Paola and Urani Chiara are co-last authors

Corresponding author:
Chiara Urani
Department of Earth and Environmental Sciences
University of Milan Bicocca
Piazza della Scienza, 1
20126 Milan Italy
Phone +390264482923
e-mail: chiara.urani@unimib.it

Abstract

Epidemiological data have linked cadmium exposure to neurotoxicity and to neurodegenerative diseases (e.g., Alzheimer's and Parkinson's disease), and to increased risk of developing ALS. Even though the brain is not a primary target organ, this metal can bypass the blood brain barrier, thus exerting its toxic effects. The coordination chemistry of cadmium is of strong biological relevance, as it resembles to zinc(II) and calcium(II), two ions crucial for neuronal signaling. A toxicogenomics approach applied to a neuronal human model (SH-SY5Y cells) exposed to cadmium (10 and 20 μM) allowed the identification of early deregulated genes and altered processes, and the discrimination between neuronal-specific and unspecific responses as possible triggers of neurodegeneration. Cadmium confirmed its recognized carcinogenicity even on neuronal cells by activating the p53 signaling pathway and genes involved in tumor initiation and cancer cell proliferation, and by down-regulating genes coding for tumor suppressors and for DNA repair enzymes. Two cadmium-induced stress responses were observed: the activation of different members of the heat shock family, as a mechanism to restore protein folding in response to proteotoxicity, and the activation of metallothioneins (MTs), involved in zinc and copper homeostasis, protection against metal toxicity and oxidative damage. Perturbed function of essential metals is suggested by the mineral absorption pathway, with *MTs*, *HMOX1*, *ZnT-1*, and *Ferritin* genes highly up-regulated. Cadmium interferes also with Ca^{2+} regulation as *S100A2* is one of the top up-regulated genes, coding for a highly specialized family of regulatory Ca^{2+}-binding proteins. Other neuronal-related functions altered in SH-SY5Y cells by cadmium are microtubules dynamics, microtubule motor-based proteins and neuroprotection by down-regulation of *NEK3, KIK15*, and *GREM2* genes, respectively.

Keywords: Cadmium; Neurotoxicity; SH-SY5Y human neuronal cells; Toxicogenomics

1. Introduction

Among the toxic metals, cadmium (Cd) is of particular concern for its environmental, chemical and biological features; it is ubiquitously distributed in the environment by natural sources (e.g. volcanic activities and forest fires), and huge anthropogenic release (~30,000 tons/year). Due to its slow excretion from the human body, and very long biological half-life (10-30 years), Cd is heavily accumulated in the organism (e.g. 2 μg/g liver, and 70 μg/g kidney) reaching its plateau in the kidney at 50 years of age. Consequently, Cd has been listed as the seventh most hazardous chemicals for human health, considering both toxicity and exposure frequency (ATDSR, 2017). Cd exposure for non-occupational reasons can primarily occur through food, drinking water, air particles, cosmetics and cigarette smoking (Bocca et al., 2014; Hartwig and Jahnke, 2017; Satarung and Moore, 2004). Being an integral constituent of tobacco with a typical content of 0.5-1 μg/cigarette, Cd is accumulated in smokers blood at concentrations 4-5 times higher than in non-smokers, and can deposit in the aortic wall of heavy smokers at concentrations up to 20 μM (Satarug and Moore, 2004).

Moreover, Cd is considered a neurotoxin, although the mechanisms remain poorly understood. One of the first evidences for a cause-effect relationship between Cd uptake and a neurodegenerative disease, was reported in 2001 in a patient with Amyotrophic Lateral Sclerosis-like syndrome after occupational Cd intoxication (Bar-Sela et al., 2001). Amyotrophic lateral sclerosis (ALS) is a progressive and invariably fatal neurodegenerative disease involving the motor system. Five to 10% of ALS cases are familial and a number of mutated genes have been identified (Aude et al., 2018), while the majority of ALS cases (90-95%) are sporadic. Despite its identification as a neurological condition 150 years ago, the etiology of motor neuron degeneration in ALS still remains largely unknown.

The general hypothesis is that sporadic ALS is a complex multi-factorial disease, and many genetic and environmental factors are under investigation as possible culprits (Ingre et al., 2015; Wang et al., 2017). Among these factors, various toxic metals and the unbalance of essential trace elements contributing to the development of ALS have been proposed: *i)* lead involvement is a long-standing hypothesis; *ii)* manganese is well known for its neurotoxic properties; *iii)* iron accumulation has been reported in ALS patients; and *iv)* the potential role of selenium has been investigated. Many other metals with potential significance for ALS have been evidenced e.g. copper, aluminium, arsenic, cobalt, zinc and cadmium, all of which have been found at elevated concentrations in ALS patients, when compared to healthy controls (Roos et al., 2013). It is noteworthy that cigarette smoking is the only factor recently identified and related to negative survival in ALS patients (Calvo et al., 2016).

Very interestingly, Cd is transported along the primary olfactory neurons to their terminations in the olfactory bulb, thereby bypassing the intact blood brain barrier, and representing therefore a likely way for Cd to reach the brain. In the nervous system, Cd tends to accumulate in the choroids plexus at concentrations much greater than those found in the cerebrospinal fluid (CSF) and in other brain areas (Wang and Du, 2013). In addition, Cd-induced apoptosis of motor neurons in cultured explants from human fetal spinal cords was observed (Sarchielli et al., 2012).

To the understanding of Cd toxic mechanisms, the coordination chemistry of cadmium(II) is of strong biological relevance as it resembles zinc(II) and calcium(II), both being crucial for neuronal signaling. Cd neurotoxicity is further described for its alterations in the release of neurotransmitters, oxidative stress, mitochondrial damage and induction of apoptosis (Maret and Moulis, 2013; Choong et al., 2014). This metal can also affect proteasomal functions and prion protein aggregation along with features responsible for axonal transport,

such as microtubule disassembly, inhibition of microtubule formation, and kinesin- and dynein-dependent motility (Böhm, 2014; Méndez-Armenta and Ríos, 2007).

However, the gathered knowledge on Cd (neuro)toxicity has not yet clarified the overall vision of the key events and processes necessary to untangle causes and consequences in a complex disease progression such as neurodegeneration.

We have applied a toxicogenomics approach to identify deregulated pathways in SH-SY5Y cells exposed to Cd, to unravel neuronal specific and non-specific responses to this toxic metal, and to recognize early genes and processes involved upon Cd exposure.

SH-SY5Y is a neuroblastoma cell line, widely used as *in vitro* model for neurotoxicity studies and neurodegenerative diseases (Cheung et al., 2009; Rossi et al., 2015). In addition, following the recommendations of the National Research Council of the National Academy of Sciences described in a recent report on toxicity testing in the 21st century, SH-SY5Y cells were used in this work as they are from human origin.

2. MATERIALS AND METHODS

2.1 Cell culture and treatments

Human SH-SY5Y neuroblastoma cells (ATCC® CRL-2266™) were cultured with Eagle Minimum Essential Medium (EMEM) and F12 medium (1:1) completed with 10% heat inactivated foetal bovine serum and 1% antibiotics (streptomycin/penicillin) at 37°C under an atmosphere of 5% CO_2 in air. All culture reagents and media were from Euroclone, Italy. Neuroblastoma cells were seeded either in 100 mm Ø Petri dish for RNA extraction at a density of $2 \cdot 10^6$ cells/dish, or in 162 cm^2 growth area flasks for SDS-PAGE and western blotting at a density of $3 \cdot 10^6$ cells/flask, with three flasks for each treatment. Twenty four hours after seeding, the cells were exposed to 10 and 20 µM $CdCl_2$ (Cd) for 48 h. The stock solution (1 mM) of $CdCl_2$ (97% purity, BDH Laboratory, Milan, Italy) was prepared in ultra-

pure water (0.22 µm filtered Milli-Q water, Millipore, Vimodrone, Milan, Italy) and stored at 4°C. Both Cd concentrations are below the cytotoxicity threshold (IC_{50}), as demonstrated by MTT assays (data not shown).

2.2. Microarray expression profiling

Total RNA was purified from SH-SY5Y cells using the RNeasy Plus kit (Qiagen). RNA was quantified using an ND-1000 UV-Vis spectrophotometer (Thermo Scientific, Wilmington, DE, USA), and the RNA integrity was assessed with the Agilent 2100 Bioanalyzer (Agilent Technologies Inc.) according to the manufacturer's instructions. The RNA samples used in this study exhibited a 260/280 ratio above 1.9 and a RNA Integrity Number (RIN) above 9.0. The microarray experiment included two biological replicates for the controls, and three for treatments. All sample-labeling, hybridization, washing, and scanning steps were conducted according to the manufacturer's specifications. Briefly, Cy3-labelled cRNA was generated from 50 ng of total RNA using the One Color Quick Amp Labeling Kit (Agilent Technologies Inc.). For every sample, 600 ng cRNA from each labeling reaction (with a specific activity above 9.0) was hybridized using the Gene Expression Hybridization Kit (Agilent Technologies Inc.) to the SurePrint G3 Human Gene Expression v2 Microarray (Agilent Technologies Inc.), an eight high-definition 60K arrays format. After hybridization, the slides were washed and then scanned with the Agilent G2565BA Microarray Scanner (Agilent Technologies Inc.). The fluorescence intensities of the scanned images were extracted and pre-processed using the Agilent Feature Extraction Software (version 10.7.3.1).

The Agilent data were processed with limma (version 3.34.9). The signal from the green channel was collected and the background subtracted using the normexp method. Normalization between arrays was performed using quantile normalization and signals from replicated spots were averaged.

153 The intensities corresponding to the same gene were also averaged and differentially
154 expressed genes were found using F-statistics implemented in limma by testing all
155 contrasts (i.e concentrations) simultaneously and adjusting for multiple tests with the
156 Benjamini and Hochberg False Discovery Rate procedure. A collection of 285 KEGG
157 pathways (release March 1, 2017) with a minimum size of 5 genes was considered for
158 EGSEA (version 1.12.0). The limma test was used to determine the log2 fold changes of
159 genes after Cd treatment. The ten methods considered for EGSEA were: camera
160 (limma:3.40.2), safe (safe:3.24.0), gage (gage:2.34.0), padog (PADOG:1.26.0), plage
161 (GSVA:1.32.0), zscore (GSVA:1.32.0), gsva (GSVA:1.32.0), ssgsea (GSVA:1.32.0),
162 globaltest (globaltest:5.38.0), fry (limma:3.40.2) (Alhamdoosh et al., 2017).

163 ***2.3 qPCR validation of transcriptomics data***

164 The total RNA was isolated using the Quick-RNATM MiniPrep (Zymo Research, Irvine, CA,
165 USA), according to manufacturer's instructions. Total RNA was reverse-transcribed using
166 SuperScript II RT (Invitrogen, Carlsbad, CA, USA), oligo dT and random primers, according
167 to the manufacturer's protocol. For quantitative real-time PCR (qPCR), SYBR Green
168 method was used to evaluate growth arrest and DNA damage-inducible protein GADD45
169 beta, heme oxygenase 1 and S100 calcium binding protein A2 expression. Briefly, 50 ng
170 cDNA was PCR amplified with Luna® Universal qPCR Master Mix (New England BioLabs,
171 Hitchin, Hertfordshire, UK) and specific primers, using an initial denaturation step at 95°C
172 for 10 min, followed by 40 cycles of 95°C for 15 sec and 59°C annealing/polymerization for
173 1 min. Each sample was normalized using β-actin gene as internal reference control. The
174 relative expression level was calculated with the Livak method (2[-ΔΔC(T)]) and expressed
175 as a relative fold change between Cd treated and untreated cells.
176 The primers used for qPCR are following: GADD45β Fw 5'-
177 CAGAAGATGCAGACGGTGAC-3' and Rv 5'-AGGACTGGATGAGCGTGAAG-3'; HMOX1

Fw 5'-TGCCCCAGGATTTGTCAGAG-3' and Rv 5'- AAGTAGACAGGGGCGAAGAC-3'; S100A2 Fw 5'- GCGACAAGTTCAAGCTGAGTA-3' and Rv 5'-ACAGTGATGAGTGCCAGGAAA-3'; β-ACT Fw 5'-CGACAGGATGCAGAAGGAG-3' and Rv 5'-ACATCTGCTGGAAGGTGGA-3'.

2.4 Cell extract preparation and immunochemical analysis of metallothioneins and heat shock proteins

2.4.1 Metallothioneins (MT)

At the end of the treatment period (48 h), cells were processed essentially according to Callegaro et al., 2018. Briefly, cells were harvested by trypsinisation, washed with ice-cold PBS, centrifugated and lysed in 10 mM Tris-HCl buffer (pH 7) containing 5mM EDTA, 1mM PMSF and protease inhibitors. All samples were immediately frozen (-20°C) to obtain cell lysates. Low molecular weight proteins, including metallothioneins (MT), were separated by high-speed centrifugation (20000 *g* for 45 min). A small aliquot of clarified samples (supernatants) was used for protein content quantification by the Bradford assay. The remaining volume of clarified samples was diluted 1:1 in sample buffer (0.25 M Tris-HCl, pH 6.8, 2% SDS, 30% glycerol, 10% β-mercaptoethanol, 0.01% bromophenol blue) and stored at -20 °C.

Total proteins (20 µg) were separated by SDS-PAGE in 12% NuPAGE gels (Invitrogen, Italy) and transferred using a transfer buffer (CAPS buffer: 10 mM 3-cyclohexylamino-1-propanesulfonic acid pH 10.8 in 10% methanol containing 2mM $CaCl_2$). Western blotting and immunoreactions were performed according to previously published protocols (Urani et al., 2010) using a mouse anti-metallothionein antibody (Zymed, Invitrogen, Corp. cat. n. 18-0133) that recognizes both MT-1 and MT-2 isoforms. Gels of the same samples were stained with Coomassie Blue for visualization of correct sample loading.

202 The expression of MT in controls and Cd-treated samples was analyzed by comparing
203 bands intensities of different samples.
204 *2.4.2. Heat shock proteins (Hsp70)*
205 Treated and control cells were collected in PBS buffer containing protease inhibitors
206 (aprotinin, leupeptin, pepstatin, PMSF), passed through a syringe needle (22-23 ga Ø) and
207 incubated on ice for 15 min. The cells were homogenized by sonication (10-15 sec on ice),
208 centrifuged, and the supernatants collected for total protein content analysis and stored at -
209 80°C in the sample buffer. Hsp70 expression was determined according to Urani and co-
210 workers (2007) by immunochemical analysis separating 30 µg of proteins on 7% Tris-
211 acetate NuPAGE gels (Invitrogen, Carlsbad, CA, USA). Separated proteins were
212 transferred onto nitrocellulose membranes, and the membranes were blocked for 2 h in
213 Tween buffer (0.1% Tween-20, 8 mM NaN_3, in PBS) containing 5% BSA. A mouse
214 monoclonal anti-hsp70 antibody (Enzo Life Sciences, Switzerland cat. ADI-SPA-810-D) was
215 used for protein detection. The protein bands were visualized after the secondary antibody
216 (goat anti-mouse phosphatase-conjugate) reaction and addition of the colorimetric
217 substrate. The equal sample loading was assessed by staining the gels of the same
218 samples with Coomassie Blue.
219 Protein levels were quantified by densitometric analysis using the Scion Image software
220 (Scion Corp., Frederick, MD, USA). Densitometric data of MT and hsp70 proteins of at least
221 three biological replicates were analyzed and the statistical comparison performed.

222 ***2.5 Statistical analysis***
223 Densitometric data from western blot and relative fold changes from qPCR were tested by
224 Dunnett's multiple comparison procedure. All calculations were conducted using the R
225 statistical programming environment. All treated samples were compared to their reference
226 controls.

3. RESULTS

3.1 Cadmium induces a strong deregulation of specific transcripts

A total of 85 genes were significantly up-regulated, and 11 genes were down-regulated (ANOVA limma, p value adjusted by the Benjamini and Hochberg's method equals or smaller than 0.05) (Smyth, 2004). The first 25 up-regulated genes are shown in Table 1 with log2 fold changes values and statistical significance (adjusted p value). Table 2 shows all down-regulated genes. The complete list and description of 96 differentially expressed genes is found in supplementary materials (Table 1S).

A major group of up-regulated genes is the metallothioneins (*MT*) family, with (sub)isoforms of *MT-1* and *MT-2* highly up-regulated (up to around 10 log2 fold change, FC) by both 10 and 20 µM Cd. MTs are proteins involved in metalloregulatory processes, and highly inducible by Zn and Cd (Choi and Bird, 2014).

HMOX1 is amongst the top up-regulated genes with *MT* in SH-SY5Y cells exposed to Cd. This gene encodes for heme-oxygenase-1 (HO-1), which is of keen research interest as it is considered to be a major protein in diseases caused by oxidative and inflammatory insults, with a role in contrasting stressful events. HO-1, which is the stress-inducible isozyme of heme oxygenase, catalyzes the breakdown of heme into free ferrous iron (Fe^{2+}), biliverdin, and carbon monoxide. Fe^{2+} stimulates the synthesis of ferritin (iron-bound-compound), biliverdin is converted to bilirubin, all being cytoprotective compounds.

A group of up-regulated and stress-related genes is represented by *ZFAND2A, HSPA1A, HSPA6, HSPA1B, DNAJB1* coding for heat shock-related proteins, belonging to a superfamily of cytoprotective chaperones, dealing with proteotoxic stress (Kostenko et al., 2014; Rossi et al., 2010).

Furthermore, the product of growth arrest and DNA damage response 45*β* (*GADD45β*) gene involved in cell growth arrest and DNA repair, and recently described as a regulatory

protein, controlling autophagy and apoptosis in rat cerebral neurons (He et al., 2016), is among the highest up-regulated genes. Another protein with pro-apoptotic properties is encoded by *DDIT3* gene, also known as CCAAT/enhancer binding homologous protein (CHOP)/GADD153 (Syk-Mazurek et al., 2017).

TEX19, AKR1C3, TGFBI, GDF15 and RRAD up-regulated genes are all coding for proteins related to cancer, cancer cell proliferation, and enhancement of tumor initiation representing, in some cases, prognostic biomarkers (see as examples Planells-Palop et al., 2017; Karunasinghe et al., 2017; Pan et al., 2018, Li et al., 2016; Yeom et al., 2014).

S100A2 is a gene coding for a member of the S100 proteins, a family of regulatory, calcium-binding-proteins that mediate signal transduction in the nervous system. S100 family members are involved in different diseases such as psoriasis, rheumatoid arthritis, cystic fibrosis, cardiomyopathy, multiple sclerosis, amyotrophic lateral sclerosis, Down's syndrome, Alzheimer's disease and cancer (Zimmer et al., 2005).

All down-regulated genes are shown in Table 2. Even though 10 µM Cd has a weak effect on gene down-regulation, it is interesting to note the trend of increasing down-regulation relevant at the highest concentration used. Analyzing all down-regulated genes, *SLC35D* is the top down-regulated with a log2 fold change of -2,15 at 20 µM Cd concentration. This gene in mouse is specifically expressed in the brain, suggesting a functional role in the central nervous system. The gene is predicted to code for an orphan nucleotide sugar transporter or a fringe connection-like protein with transmembrane domains (Zhang et al., 2014). Another down-regulated gene related to transporter functions is *SLC39A10*. This gene encodes for a member of the Zip proteins, a family of import Zn^{2+} transporters (Landry et al., 2019).

GALNT6 encodes for the polypeptide *N*-acetylgalactosaminyltransferase 6, critical for the stability, subcellular localization, and anti-apoptotic function of GRP78 protein in cancer cells (Lin et al., 2017).

Little is known about *GLCCI1,* glucocorticoid-induced transcript 1, in the central nervous system, recently proposed as a tool to identify progenitors in the ventricular zone during telencephalon development (Kohli et al., 2018). Even though the general functions of this gene are unclear, this cortical-response gene plays a role in regulating the sensitivity to endogenous cortisol in humans (Liu et al., 2017 and references therein).

Very interestingly, among the down-regulated genes, a group of Cd-targeted genes encodes for neuronal-related proteins: *GREM2* codes for a member of the gremlin protein family, described as neuroprotective factors in dopaminergic neurons both *in vivo* and *in vitro* (Phani et al., 2013); the product of *Nek3* influences neuronal morphogenesis and polarity through effects on microtubules as this protein belongs to a Ser/Thr kinases involved in coordinating microtubule dynamics (Chang et al., 2009); *Kif15* product belongs to the kinesins superfamily of microtubule-based motor proteins, particularly expressed in neurons undergoing migration and in the developing brain (Klejnot et al., 2014).

Finally, a group of down-regulated genes produces transcripts related to carcinogenesis: *UNG*, that encodes for uracil-DNA glycosylase protein responsible for the initial step in the base excision repair pathway (Gokey et al., 2016); *PDGFRL*, the platelet-derived growth factor receptor-like gene is regarded as a tumor suppressor, although the precise biological function is not known (Kawata et al., 2017); *TXNIP* gene encodes for a potent tumor suppressor protein, and its down-regulation leads to increase proliferation of certain types of cancer cells (Park et al., 2018).

Table 1

Top up-regulated genes in SH-SY5Y cells treated with 10 or 20 μM Cd for 48 h

Gene	Cd10 μM log2 fold change	Cd20 μM log2 fold change	adj.P.Value	Description
MT1M	9,71	9,92	2,61E-05	metallothionein 1M
MT1X	7,11	7,53	7,53E-05	metallothionein 1X
MT1F	7,10	7,37	8,98E-05	metallothionein 1F
MT1L	7,04	7,43	3,84E-05	metallothionein 1L (gene/pseudogene)
MT1HL1	6,95	7,42	3,84E-05	Metallothionein 1H-like protein 1
MT1B	6,74	7,25	2,61E-05	metallothionein 1B
ENST00000567054	6,63	7,02	3,84E-05	metallothionein 1C (pseudogene)
HMOX1	6,08	7,26	0,001731748	heme oxygenase (decycling) 1
MT2A	5,42	5,45	0,000160204	metallothionein 2A
MT1A	4,92	5,29	0,00014948	metallothionein 1A
GADD45β	4,82	7,05	0,000545108	growth arrest and DNA-damage-inducible, beta
MT1E	3,95	4,15	0,000250941	metallothionein 1E
ZFAND2A	3,64	5,20	0,006524353	zinc finger, AN1-type domain 2A
TEX19	3,47	4,15	0,003753672	testis expressed 19
GDF15	3,24	4,22	0,002993824	growth differentiation factor 15
AKR1C3	2,94	3,14	0,002993824	aldo-keto reductase family 1, member C3 (3-alpha hydroxysteroid dehydrogenase, type II)
TGFBI	2,90	3,59	0,013115332	transforming growth factor, beta-induced, 68kDa
MT1G	2,70	3,36	0,034682665	metallothionein 1G
HSPA1A	2,67	4,38	0,005651168	heat shock 70kDa protein 1A
HSPA6	2,53	4,36	0,000545108	heat shock 70kDa protein 6 (Hsp70B')
RRAD	2,53	4,24	0,00208082	Ras-related associated with diabetes
HSPA1B	2,29	4,10	0,014428639	heat shock 70kDa protein 1B
DNAJB1	2,23	3,57	0,001731748	DnaJ (Hsp40) homolog, subfamily B, member 1
DDIT3	2,21	3,45	0,000545108	DNA-damage-inducible transcript 3
S100A2	1,98	2,91	0,001731748	S100 calcium binding protein A2

Table 2

Complete list of down-regulated genes in SH-SY5Y cells treated with 10 or 20 μM Cd for 48 h.

Gene	Cd10 μM log2 fold change	Cd20 μM log2 fold change	adj.P.Value	Description
SLC35D3	-1,41	-2,15	0,03018534	solute carrier family 35, member D3
GREM2	-1,02	-1,32	0,02198818	gremlin 2
SLC39A10	-0,88	-1,07	0,04704006	solute carrier family 39 (zinc transporter), member 10
GLCCI1	-0,84	-1,42	0,02971039	glucocorticoid induced transcript 1
GALNT6	-0,82	-1,48	0,03741771	UDP-N-acetyl-alpha-D-galactosamine:polypeptide N-acetylgalactosaminyltransferase 6 (GalNAc-T6)
NEK3	-0,77	-1,28	0,04518064	NIMA (never in mitosis gene a)-related kinase 3
UNG	-0,72	-1,00	0,04826738	uracil-DNA glycosylase
TXNIP	-0,65	-1,77	0,01403976	thioredoxin interacting protein
LOC642366	-0,53	-1,24	0,04997033	uncharacterized LOC642366
PDGFRL	-0,51	-1,53	0,02586179	platelet-derived growth factor receptor-like
KIF15	-0,42	-1,09	0,03768701	kinesin family member 15

3.2 Most deregulated genes show a concentration-dependence profile

All deregulated genes and their trends are shown in Figure 1. The ninety-six differentially expressed genes (p adj ≤ 0.05, ANOVA limma) in Cd-treated *vs* control samples are shown in the heat map of Figure 1A. After clustering these significant genes, a first cluster of 11 highly down-regulated genes (*SLC35D3*, *PDGFRL*, *TXNIP*, *KIF15*, *LOC6442366*, *UNG*, *SLC39A10*, *GREM2*, *NEK3*, *GALNT6* and *GLCCI1*) was observed. A second cluster of 11 strongly up-regulated genes (*MT1X*, *MT1F*, *MT1L*, *MT1HL1*, *MT1B*, *MT1A*, *MT2A*, *MT1M*, GADD45β, *HMOX1* and *ENST00000567054*) was also found. In addition to these highly significant genes, a third cluster was made of 74 genes found to be up-regulated with lower log2 fold changes (Figure 1A).

It is worth noting that a Cd concentration-dependence was observed for most of these 96 deregulated genes (Figure 1B). The highest Cd concentration tested (i.e 20 µM) resulted in a more pronounced log2 fold change when compared to 10 µM Cd-treatment. When using a cut-off at an absolute log2 fold change of 3 (for any of the two tested concentrations), the highly significant genes in clusters 1 and 2 (Figure 1A) showed such concentration-dependence (Figure 1B). In addition, 15 up-regulated genes from cluster 3 also showed a concentration-dependence profile (namely, *MT1E*, *MT1G*, *HSPA1A*, *HSPA1B*, *HSPA6*, *ZFAND2A*, *RRAD*, *GDF15*, *TEX19*, *MLC1*, *TGFBI*, *DNAJB1*, *ZNF165*, *DDIT3* and *AKRC3*).

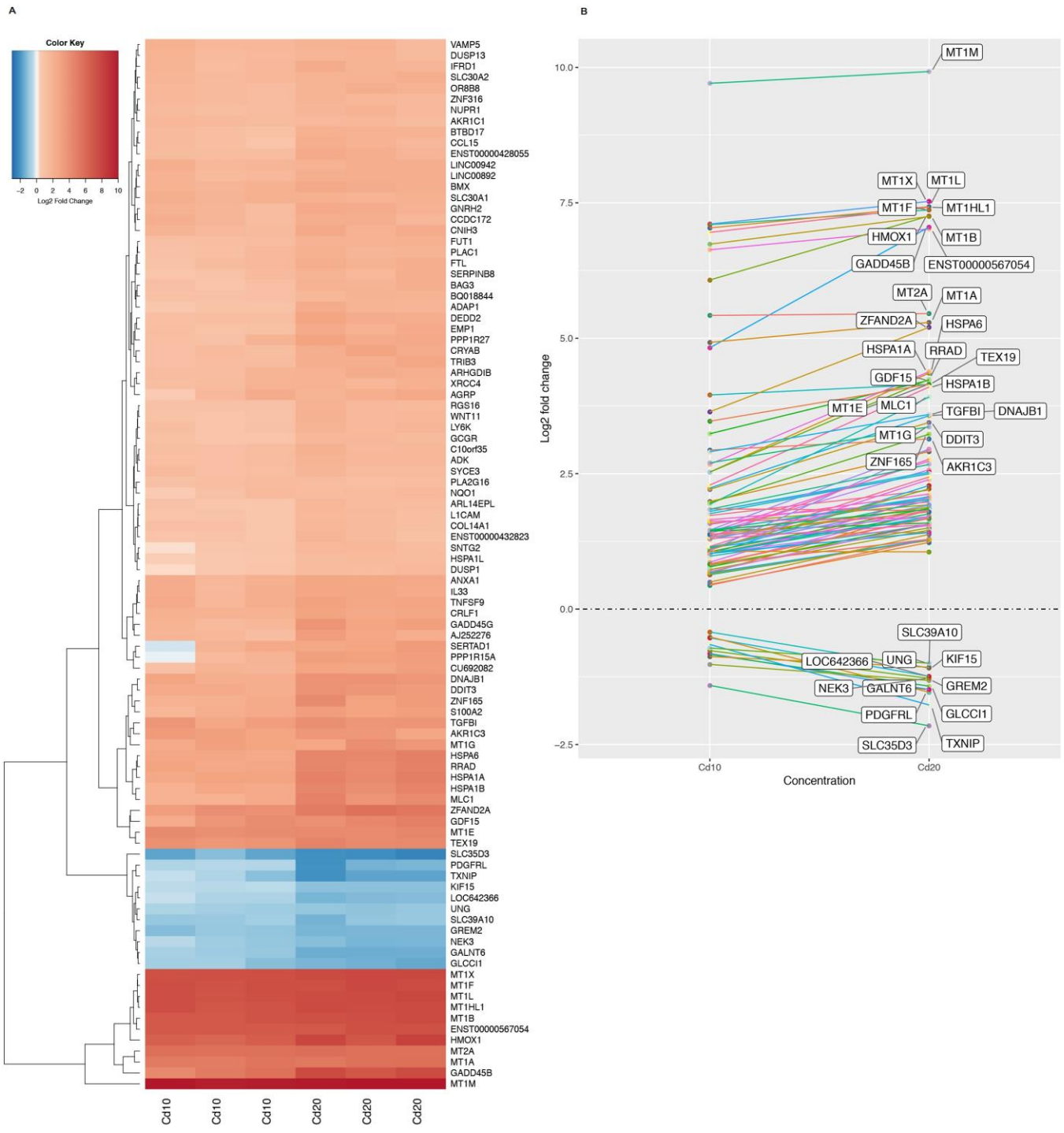

327

328

329 **Figure 1**

330 **Toxicogenomics analysis of cadmium on SH-SY5Y cells**

331 **(A) Heatmap of differentially expressed genes after cadmium treatment**

332 The log2 fold changes of differentially expressed genes (p adj ≤ 0.05, ANOVA-limma
333 adjusted for multiple comparisons according to the Benjamini-Hochberg method), are
334 represented in the heatmap for three replicates of Cd-treated samples (10 and 20 µM 48 h).

Red color represents up-regulated genes when compared to control conditions, whereas blue color is used for down-regulated genes. The gene names are shown on the right side of the heatmap and the treatment conditions are indicated at the bottom part. On the left, the hierarchical clustering of the genes (see the text for details).

(B) Dose dependence of 96 differentially expressed genes

The log2 fold changes of the ninety-six genes found to be differentially expressed after cadmium treatment (p adj ≤ 0.05, ANOVA-limma) are plotted, with the cadmium concentration on the x-axis and the log2 fold change on the y-axis. Each line connects the log2 fold changes observed at the two concentrations tested (10 and 20 µM). The name of genes with an absolute log2 fold change that are higher than 3, are indicated, corresponding to eleven down-regulated and twenty-six up-regulated genes. The up-regulated genes are separated from the down-regulated genes by a horizontal dashed line at log2 fold change = 0.

3.3. Mineral absorption, cancer related and glycosphingolipid biosynthesis pathways are the main pathways perturbed by cadmium

Ensemble of Gene Set Enrichment Analyses (EGSEA) was applied to determine the KEGG pathways perturbed by Cd treatment. At 10 µM, the five most important pathways, as determined by their low median ranks across ten methods performed by EGSEA, were: p53 signaling pathway, mineral absorption, glycosphingolipid biosynthesis, basal cell carcinoma and endometrial cancer (p adj ≤ 0.05, Wilcoxon rank sum test adjusted by the Benjamini and Hochberg's procedure) (Figure 2A). The individual ranks attributed to the KEGG pathways by each method are reported in Supplementary Table 2S.

At 20 µM Cd, the seven most perturbed KEGG pathways were: Fanconi anemia pathway, mineral absorption, p53 signaling pathway, legionellosis, rheumatoid arthritis, homologous recombination and glycosphingolipid biosynthesis (Figure 2B). The ranks of the KEGG pathways are detailed in Supplementary Table 3S.

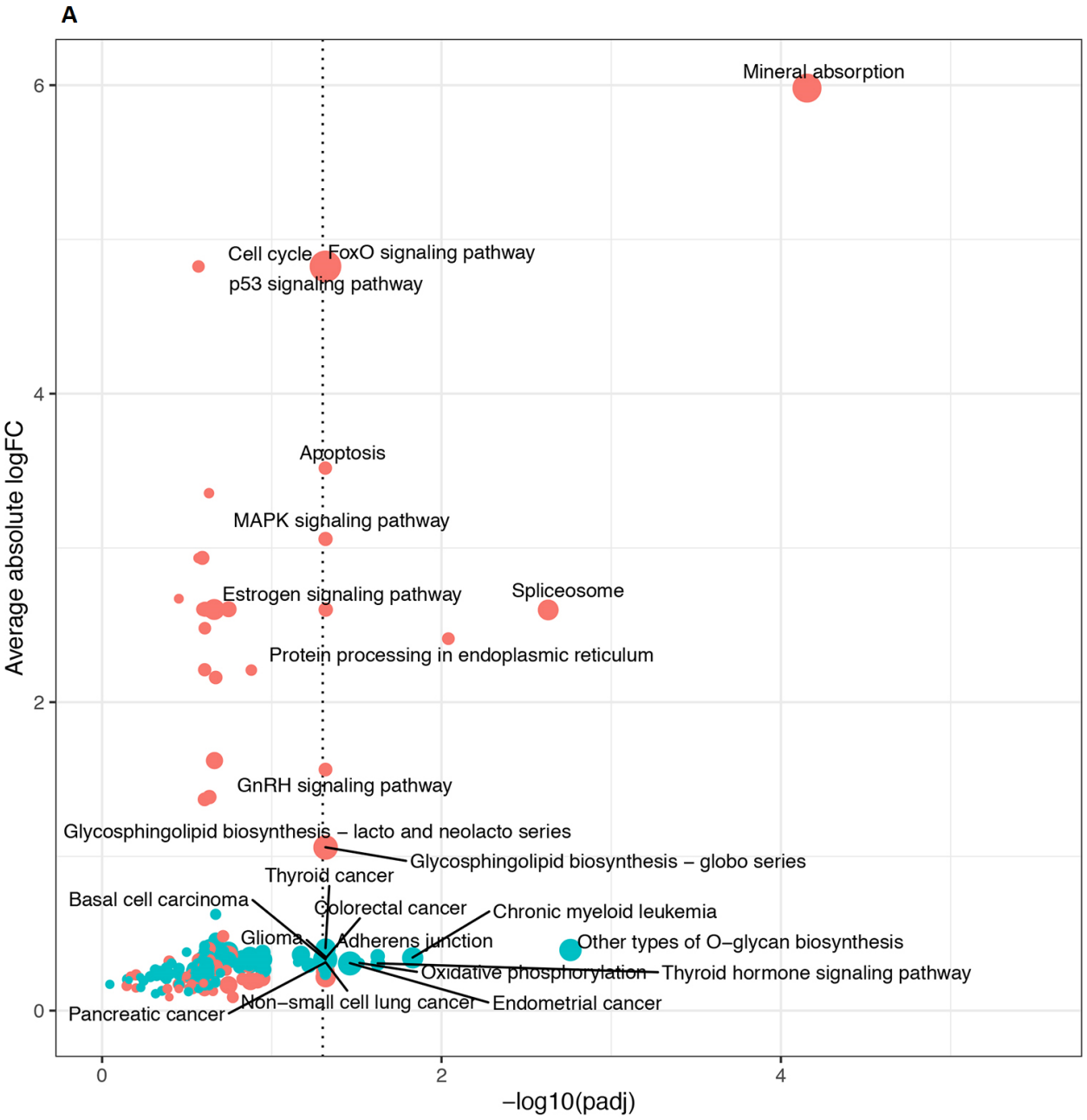
A
Mineral absorption
Cell cycle
FoxO signaling pathway
p53 signaling pathway
Apoptosis
MAPK signaling pathway
Estrogen signaling pathway
Spliceosome
Protein processing in endoplasmic reticulum
GnRH signaling pathway
Glycosphingolipid biosynthesis – lacto and neolacto series
Glycosphingolipid biosynthesis – globo series
Thyroid cancer
Basal cell carcinoma
Colorectal cancer
Chronic myeloid leukemia
Glioma
Adherens junction
Other types of O–glycan biosynthesis
Oxidative phosphorylation
Thyroid hormone signaling pathway
Non–small cell lung cancer
Endometrial cancer
Pancreatic cancer
Average absolute logFC
–log10(padj)
0
2
4
6
0
2
4

362

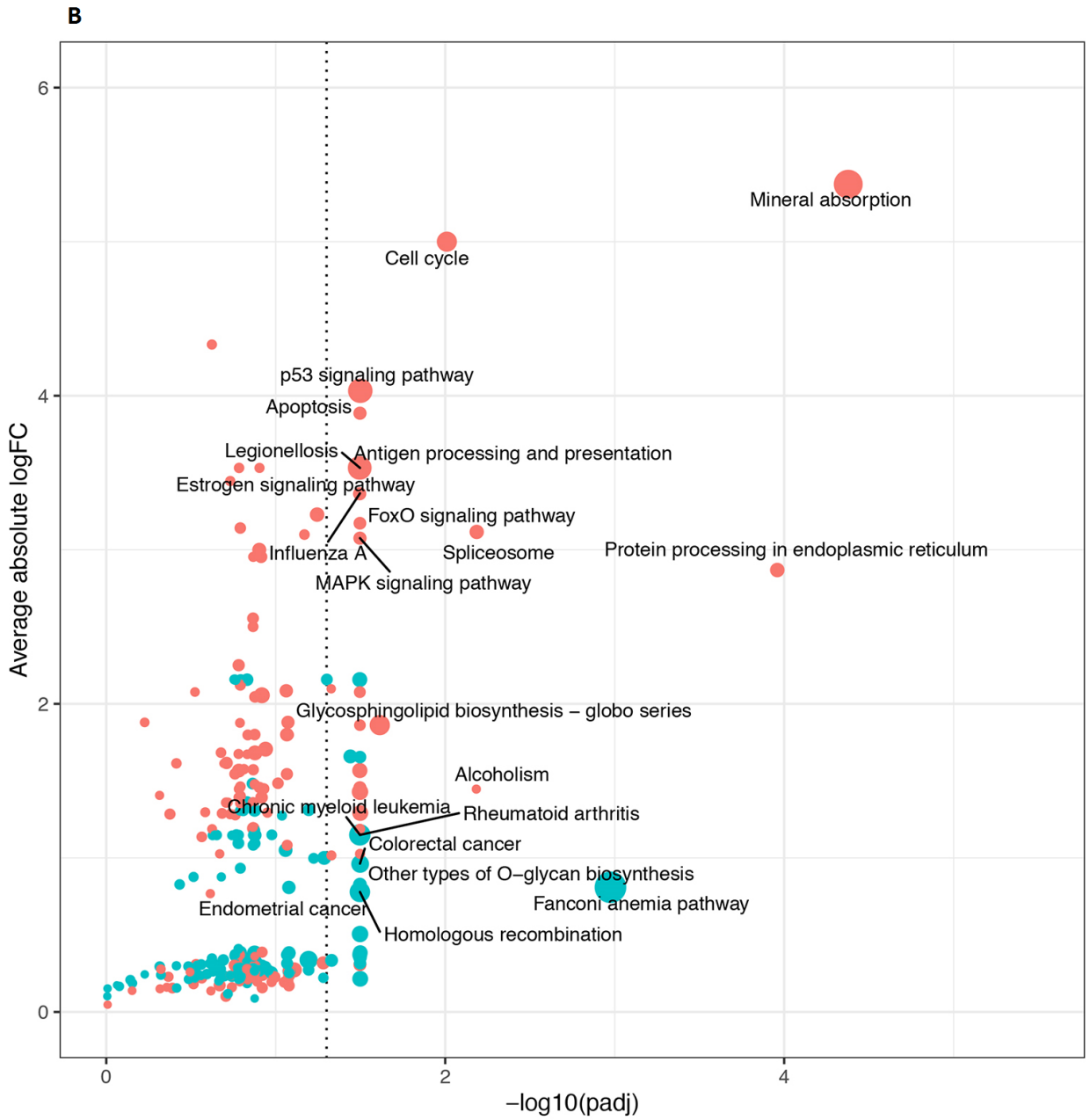

Figure 2

EGSEA of KEGG pathways after cadmium treatment

The x-axis shows the -log10 of the EGSEA Wilcoxon p value adjusted for multiple comparisons of the KEGG pathways, and the y-axis represents the average of the absolute log2 fold changes of the genes present in each of these pathways. A collection of 285 KEGG pathways with a minimum size of 5 genes was considered for EGSEA. The limma test was used by EGSEA to determine the log2 fold changes of genes after treatment with 10 (panel **A**) or 20 (panel **B**) µM of cadmium. A bigger dot is used for KEGG pathways of lower median ranks observed across ten methods performed by EGSEA. The vertical dashed line at -log10 (padj) = 1.3 corresponds to a false discovery rate of 0.05. Red color is used for up-regulated KEGG pathways whereas blue color represents down-regulated pathways.

Three KEGG pathways are in common when comparing the two Cd concentrations used. The path views for these three pathways: mineral absorption, p53 signaling pathway and glycosphingolipid biosynthesis, highlight some important genes that are altered by Cd (Figure 3). For the mineral absorption, the up-regulation of metallothioneins (*MT1 and MT2 isoforms*), HMOX (*HMOX1*), ZnT1 (*SLC30A1*), Zip4 (*SLC39A4*) and ferritin heavy chain 1 (*FTH1*) was observed whereas down-regulation of heme carrier protein 1 (*HCP1/SLC46A1*) and ferroportin (*FPN1/SLC40A1*) was found (Figure 3A).

In the p53 signaling pathway, there is up-regulation of Gadd45 (*GADD45A/B/G*), p21 (*CDKN1A*), Noxa (*PMAIP1*) and the Sestrins (*SESN2*) (Figure 3B). In addition to *p21*, *CDK6* is another gene present in the cell cycle module of the p53 signaling pathway and found to be down-regulated. When looking at the cell cycle pathway itself, we observed down-regulation of additional genes such as *EP300*, *MCM* (2 to 10), and *E2F* (1 to 8) (Supplementary Figure 1S). The importance of cancer related pathways is further highlighted by the endometrial cancer pathway, containing the p53 signaling and cell cycle modules but also the PI3K-Akt signaling pathway. In this latter pathway, there was down-regulation of PI3K (*PIK3CA*) and PKB (*AKT1*) (Supplementary Figures 1S). Of interest, the homologous recombination pathway was also found significant, driven by down-regulation of *RAD50*, *RAD51* and *RAD54L* subunits, and of the catalytic subunit of DNA polymerase epsilon (*POLE*) (Supplementary Figure 1S). Another cancer related pathway, i.e basal cell carcinoma, was also revealed by EGSEA. This pathway contains the p53 signaling and the cell cycle modules, but also the Wnt signaling pathway (Supplementary Figure 1S). In this pathway, Wnt (*WNT2, 7A, 8A, 10B, 11*) were up-regulated after Cd treatment, whereas Frizzled (*FZD1*), TCF/LEF (*TCF7, TCF7L1, TCF4, LEF1*) were down-regulated.

In the glycosphingolipid biosynthesis pathway, we found up-regulation of fucosyltransferase 1 (*FUT1*/ KEGG enzyme 2.4.1.69), beta-hexoaminidase (*HEXA* and *HEXB*, KEGG enzyme

3.2.1.52) and alpha-galactosidase (*GLA*/KEGG enzyme 3.2.1.22). This large group of complex lipids is particularly abundant in the outer layer of neuronal plasma membranes. (See Figure legend on pag. 24)

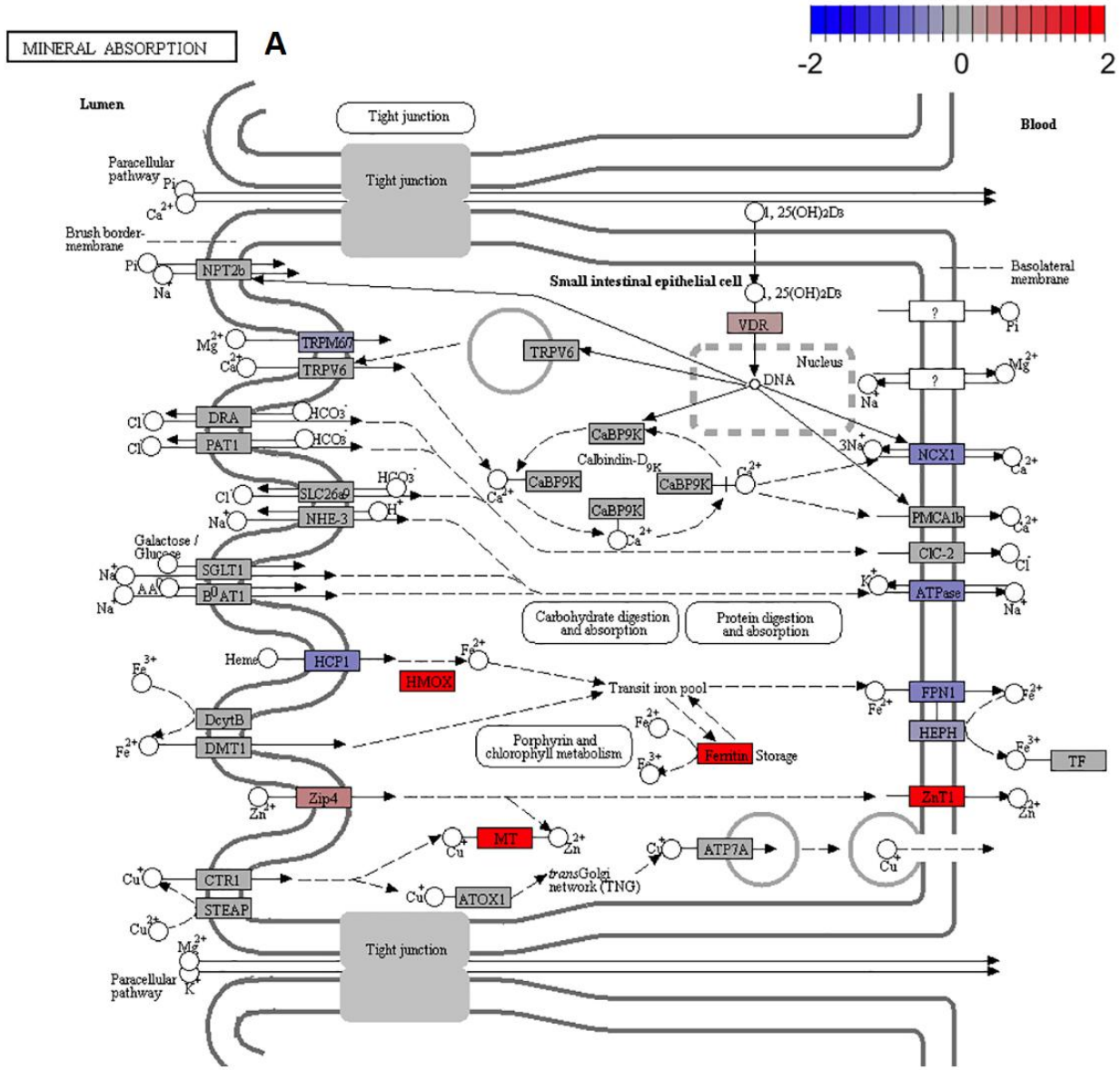

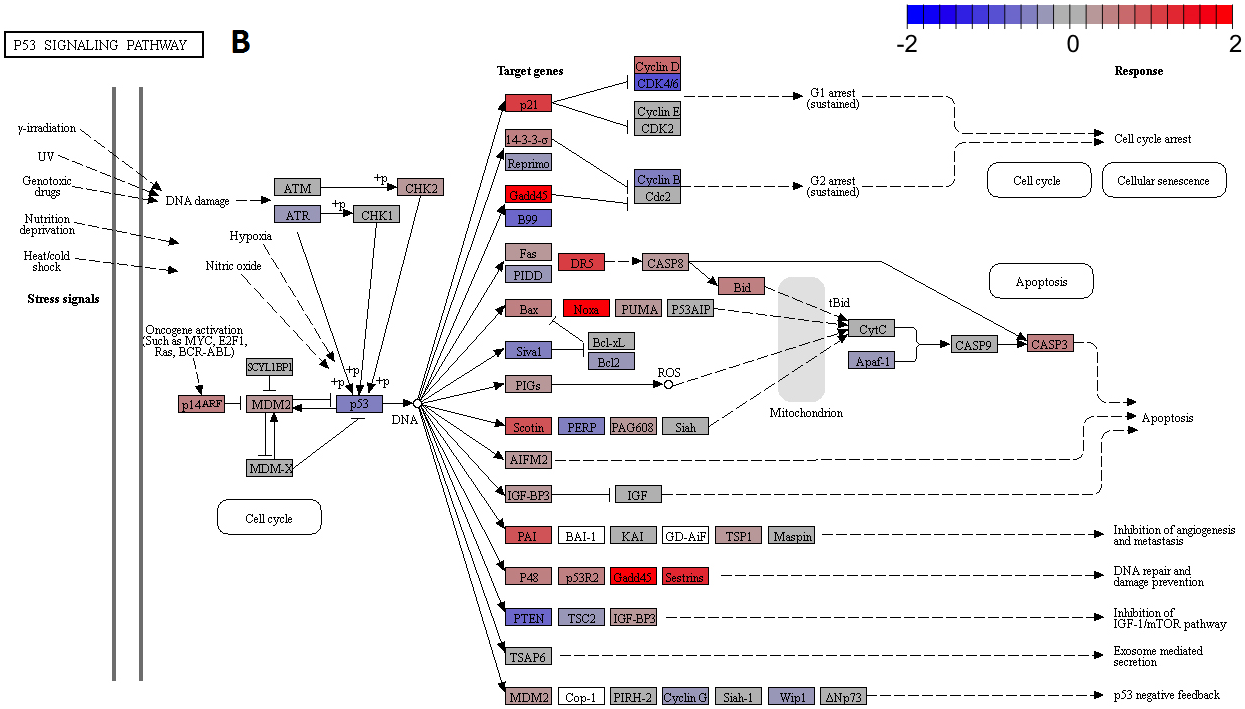
P53 SIGNALING PATHWAY
B
-2
0
2
Target genes
Response
Stress signals
γ-irradiation
UV
Genotoxic drugs
Nutrition deprivation
Heat/cold shock
DNA damage
ATM
ATR
CHK2
CHK1
Hypoxia
Nitric oxide
Oncogene activation (Such as MYC, E2F1, Ras, BCR-ABL)
3CYL1BP1
p14ARF
MDM2
p53
MDM-X
DNA
Cell cycle
p21
14-3-3-σ
Reprimo
Gadd45
B99
Cyclin D
CDK4/6
Cyclin E
CDK2
Cyclin B
Cdc2
G1 arrest (sustained)
G2 arrest (sustained)
Cell cycle arrest
Cell cycle
Cellular senescence
Fas
PIDD
DR5
CASP8
Bid
Apoptosis
Bax
Noxa
PUMA
P53AIP
tBid
Sival
Bcl-xL
Bcl2
CytC
Apaf-1
CASP9
CASP3
PIGs
ROS
Mitochondrion
Scotin
PERP
PAG608
Siah
Apoptosis
AIFM2
IGF-BP3
IGF
PAI
BAI-1
KAI
GD-AiF
TSP1
Maspin
Inhibition of angiogenesis and metastasis
P48
p53R2
Gadd45
Sestrins
DNA repair and damage prevention
PTEN
TSC2
IGF-BP3
Inhibition of IGF-1/mTOR pathway
TSAP6
Exosome mediated secretion
MDM2
Cop-1
PIRH-2
Cyclin G
Siah-1
Wip1
ΔNp73
p53 negative feedback

408

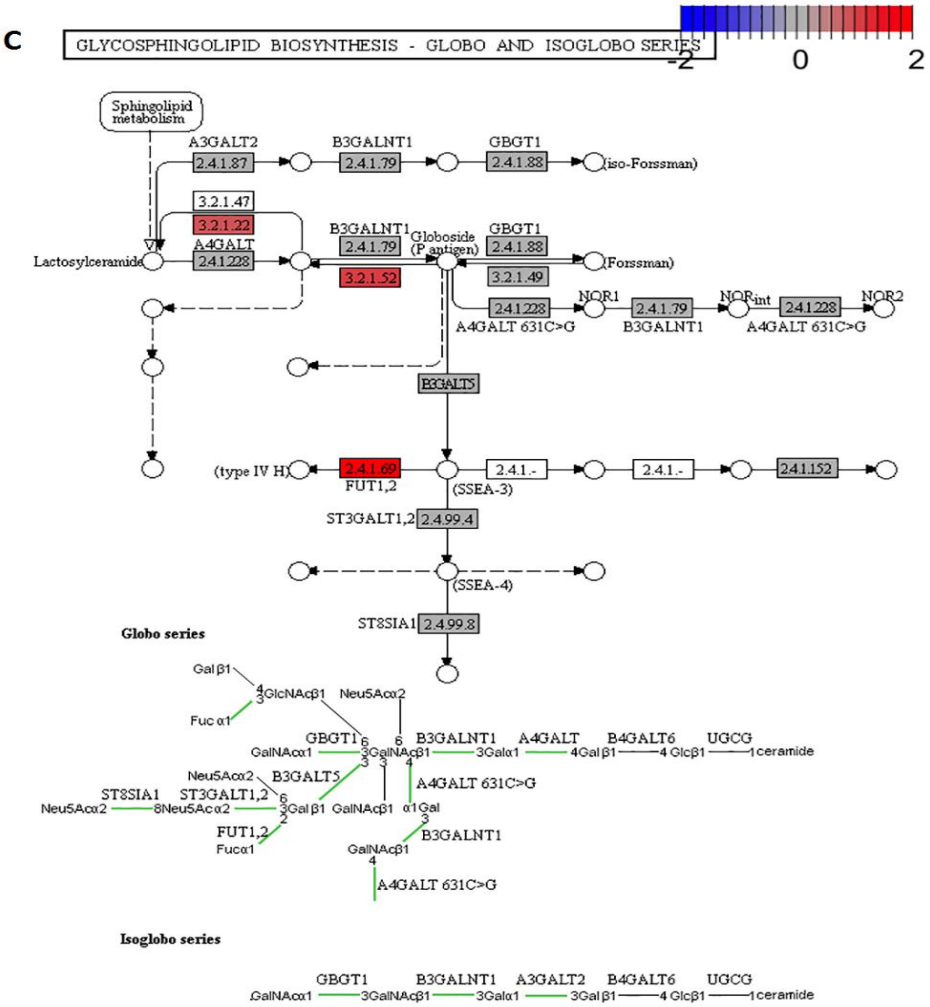
C
GLYCOSPHINGOLIPID BIOSYNTHESIS - GLOBO AND ISOGLOBO SERIES
-2
0
2
Sphingolipid metabolism
A3GALT2
2.4.1.87
B3GALNT1
2.4.1.79
GBGT1
2.4.1.88
(iso-Forssman)
3.2.1.47
3.2.1.22
A4GALT
2.4.1.228
Lactosylceramide
B3GALNT1
2.4.1.79
Globoside (P antigen)
GBGT1
2.4.1.88
(Forssman)
3.2.1.52
3.2.1.49
2.4.1.228
A4GALT 631C>G
NOR1
2.4.1.79
B3GALNT1
NOR int
2.4.1.228
A4GALT 631C>G
NOR2
B3GALT5
(type IV H)
2.4.1.69
FUT1,2
2.4.1.-
(SSEA-3)
2.4.1.-
2.4.1.152
ST3GALT1,2
2.4.99.4
(SSEA-4)
ST8SIA1
2.4.99.8
Globo series
Gal β1
4
3
GlcNAc β1
Neu5Ac α2
Fuc α1
GBGT1
GalNAc α1
6
3
3
GalNAc β1
B3GALNT1
3Gal α1
A4GALT
4Gal β1
B4GALT6
4 Glc β1
UGCG
1 ceramide
Neu5Ac α2
B3GALT5
A4GALT 631C>G
ST8SIA1
Neu5Ac α2
ST3GALT1,2
8Neu5Ac α2
6
3
3Gal β1
GalNAc β1
α1Gal
3
2
FUT1,2
Fuc α1
B3GALNT1
GalNAc β1
4
A4GALT 631C>G
Isoglobo series
GBGT1
GalNAc α1
B3GALNT1
3GalNAc β1
A3GALT2
3Gal α1
B4GALT6
3Gal β1
4 Glc β1
UGCG
1 ceramide

409

Figure 3
Path views of three significant KEGG pathways altered by 20 µM of cadmium
The comparison of microarray data between cells treated with 20 µM of cadmium and controls was made using limma. The mineral absorption (**A**), p53 signaling pathway (**B**), and glycosphingolipid biosynthesis pathway (**C**), are shown with the log2 fold changes of genes layered onto the native KEGG pathway views. A red color illustrated up-regulated genes whereas blue represents down-regulated genes, when compared to control cells.

Overall, the EGSEA shows that Cd is targeting three important pathways (mineral absorption, p53 signaling and glycosphingolipid biosynthesis pathways), with "mineral absorption" likely representing the most direct effects of Cd on human neuronal cells.

3.4 Metallothioneins and the heat shock response are the earliest cytoprotective mechanisms against cadmium

MT-I and –II are highly inducible isoforms of cytoprotective proteins, as clearly demonstrated by our transcriptomics data (see Table 1) and protein expression (Figure 4). Western blots, followed by densitometric analyses of MT-I and –II protein levels revealed a strong a dose-dependent increase with 25 and 40 mean fold changes after treatment with 10 and 20 µM Cd, respectively (Figure 4).

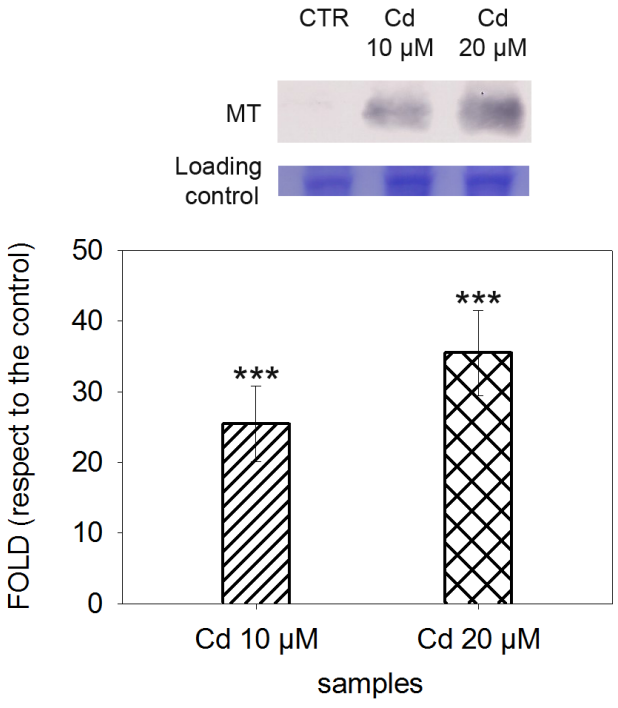

Figure 4
Metallothioneins expression in cadmium-treated SH-SY5Y cells
Metallothionein (MT-I, -II) expression (**A**) is highly induced in SH-SY5Y cells exposed to 10 and 20 μM Cd for 48 h. Very low, undetectable levels of MT are present in the controls (CTR), whereas Cd treated cells show a dose-dependent increase of protein expression, confirmed by the relative protein expression measured by densitometry analyses (**B**). ***Significantly different from control ($p<0.001$) (Dunnett's test).

We observed a similar response for Hsp70, which represents one of the highly conserved and inducible heat shock family members. As for MTs, Hsp70 protein expression (Figure 5) follows a dose-dependent pattern. In accordance with previous data (Kostenko et al., 2014), showing that members of DNAJ/Hsp40 family are involved in recruiting chaperone Hsp70, we found *DNAJB1*, a *DNAJ/Hsp40 homolog*, to be upregulated following treatment with both 10 and 20 μM Cd (see par. 3.1, and Table 1).

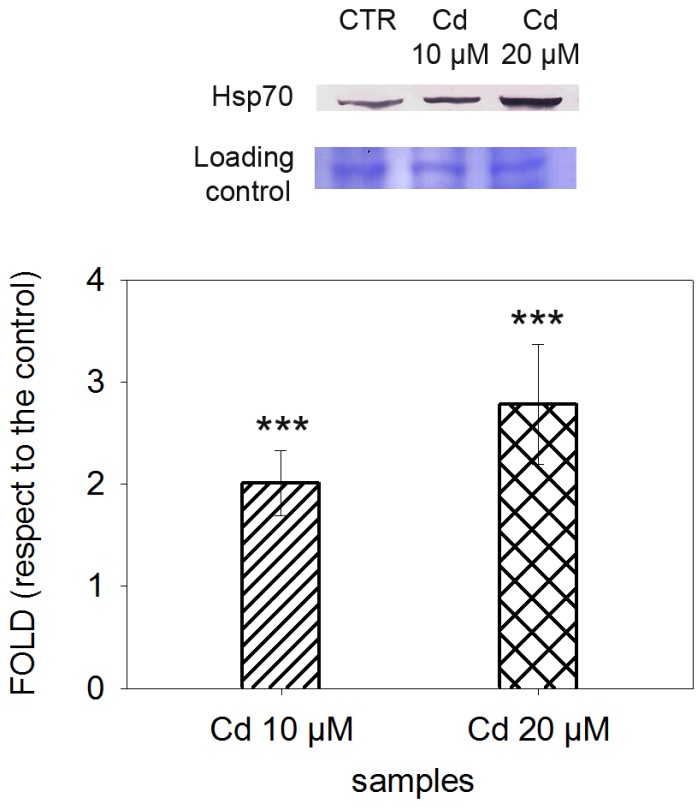

Figure 5
Heat shock protein 70 expression in cadmium-treated SH-SY5Y cells
(A) High constitutive levels of Hsp70 are present in controls (CTR), and are increased by Cd treatment (10 and 20 μM). **(B)** The increased expression is confirmed by densitometry analysis and reveals a significant difference between CTR and treated samples. ***Significantly different from control ($p<0.001$) (Dunnett's test).

In addition, the expression of *GADD45β*, *HMOX-1*, and *S100A2* genes assessed by qPCR (Figure 6), strongly supports and validates transcriptomics results, showing an increased expression of both *GADD45β*, *HMOX-1* and, to a less extent, of *S100A2 mRNA.*

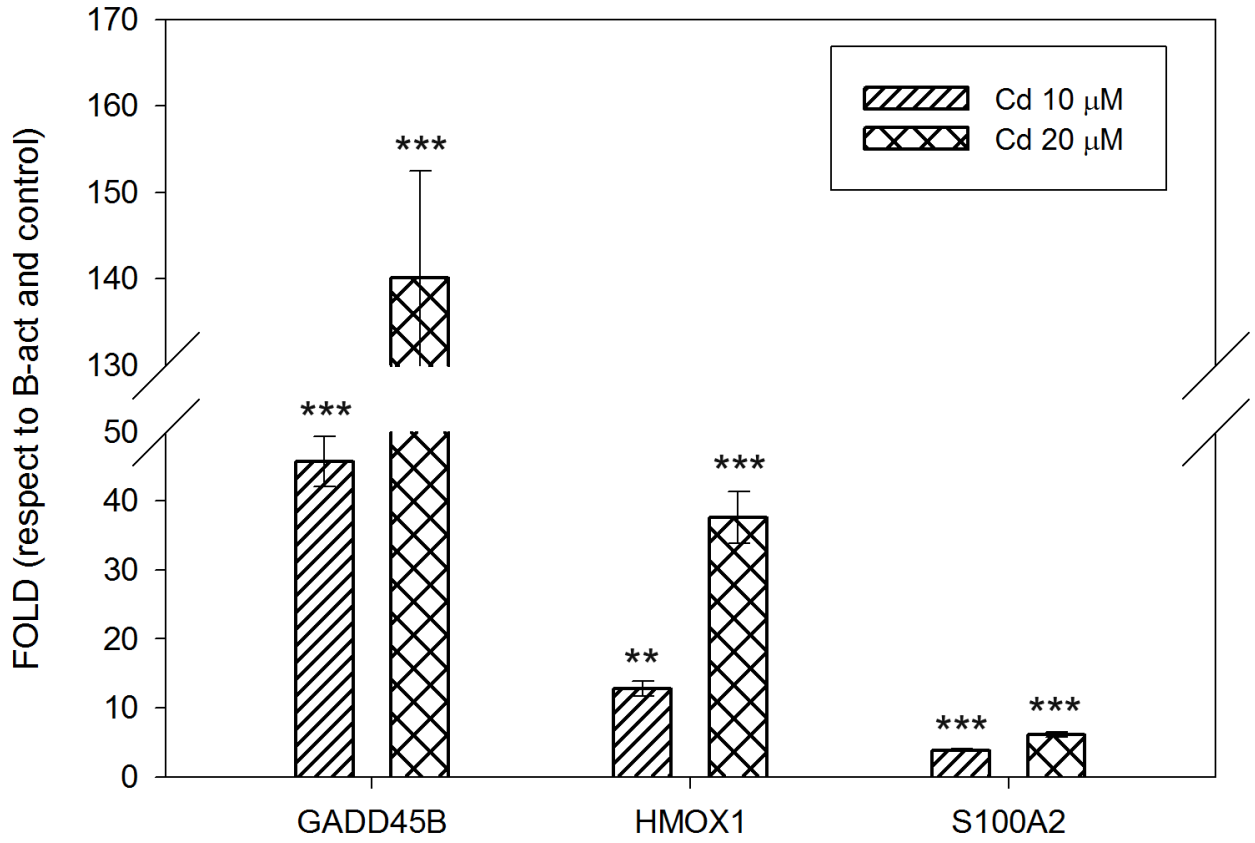

Figure 6
Relative quantification of GADD45β, HMOX1 and S100A2 mRNA levels by real time quantitative PCR. The relative expression levels were expressed as a fold change ± SE, using β-ACT gene as internal reference control and SHSH5Y cells not treated with Cd (control) as calibrator. Values are presented as means of three different experiments.
** Significantly different from control ($p<0.01$); ***significantly different from control ($p<0.001$) (Dunnett's test).

4. DISCUSSION AND CONCLUSIONS

Epidemiological and experimental studies have linked cadmium exposure to impaired functions of the nervous system and to neurodegenerative diseases, such as Alzheimer's disease and Parkinson's disease (Wang and Du, 2013), and to increased risk of developing ALS (Wang et al., 2017; Sheykhansari et al., 2018). However, its involvement in neurodegeneration and neurodegenerative-related mechanisms has been highly neglected, despite the increasing number of papers referring to Cd toxic effects on the neuronal system. Our results on SH-SY5Y cells, a human neuronal model, provide the evidence of neurotoxic mechanisms of cadmium, which could represent key triggers in the neurodegenerative process.

This toxic metal is widely studied to unravel the mechanisms for its carcinogenicity (see for example Chen et al., 2019; Fabbri et al., 2012; Forcella et al., 2016; Hartwig, 2018). Our results on human SH-SY5Y neuronal cells confirm that cadmium induces the expression of genes belonging to a carcinogenic effect even on brain derived cells. These cells respond to Cd exposure by activating e.g., the p53 signaling pathway, involved in cell cycle arrest upon stress signals and associated with cancer (see for example Joerger and Fersht, 2016), and genes involved in tumor initiation and cancer cell proliferation (*TEX19, AKR1C3, TGFB1,* and *RRAD)*, or down-regulating tumor suppressors (*PDGFRL, TXNIP*), or enzymes involved in the initial step of DNA repair (*UNG*). All these conditions create an environment susceptible to carcinogenesis.

The SH-SH5Y neuronal cells exposed to Cd respond to the metal-induced stress by activating two major defense mechanisms, namely the heat shock proteins (Hsp), and the metallothioneins (MT). Both MT and Hsp represent the first line of defense against cadmium and metals in general. Multiple functions, including the involvement of Zn and Cu homeostasis, protection against metal toxicity and oxidative damage, are associated to MT

(Babula et al., 2012). The heat shock response has evolutionary evolved as a cell defense mechanism to maintain proteostasis and restore perturbed protein homeostasis. The Hsp are mainly involved in the assistance of refolding or degrading intracellular proteins injured upon stress. The modulation of these defense mechanisms is a response evidenced in mammalian cells, both in cadmium target (e.g., hepatic, kidney and bronchial cell models) and in non-target tissues, such as Sertoli and brain cells (Bonham et al., 2003; Han et al., 2007; Hung et al., 1998; Luparello et al., 2011; Kusakabe et al., 2008; Urani et al., 2007, 2010). The high response of different family members of heat shock proteins, visualized both as increased protein (Hsp70) expression and as transcripts (*HSPA1A*, *HSPA6*, *HSPA1B*, *DNAJB1*) in our samples exposed to cadmium, shows the need of these molecular chaperones to refold mis-folded proteins and/or degrade damaged or aggregated ones. The perturbation of protein homeostasis and protein folding, aggregation and degradation may lead to accelerated ageing and the incidence of proteotoxicity-triggered disorders, all hallmarks of a number of neurodegenerative diseases, including ALS (Barna et al., 2018; Kalmar et al., 2014). In addition, many proteins arising and/or aggregating during neurodegeneration include, among others, beta-amyloid, tau and heat shock proteins, which act as danger-associated molecular patterns that compromise neuronal functions and cause cell death (Ardura-Fabregat et al., 2017).

MT are Zn-bound low molecular weight proteins (<7 KDa), which have a major role in the maintenance of metal homeostasis, mainly Zn and Cu, with their α- and β-cluster domains responsible for the binding of up to seven metals. The Zn-bound form of MT is an anti-oxidant agent, as the Zn-sulphur cluster is sensitive to changes in the redox state, thus having also a protective role against reactive oxygen species. Zn, after iron, is the second most abundant metal in organisms, playing pivotal roles as structural, catalytic, and signaling component, and as a modulator of synaptic activity and neuronal plasticity. Thus,

518 due to the relative abundance of Zn in the brain, which is protein-bound or
519 compartmentalized to be maintained at very low concentrations, MT are also expected to
520 regulate the intracellular Zn pools in the brain. This function is coordinated with two zinc
521 transporter families, Zrt- and Irt-like proteins (SLC39A), and Zn transporters (ZnT family
522 members) (Méndez-Armenta and Rìos, 2007; Prakash et al., 2015; Kimura and Kambe,
523 2016). In our model of SH-SY5Y neuronal cells, the highly dose-dependent up-regulation of
524 MT-I and –II proteins represents the immediate response to Cd exposure. In addition, the
525 mineral absorption pathway is the one most significantly perturbed by both Cd
526 concentrations used. Notably, highly up-regulated genes in this pathway are represented by
527 *MTs*, *HMOX1*, *Ferritin*, and *ZnT-1*. The membrane protein encoded by *ZnT-1* gene belongs
528 to a family of Zn transporters, specifically responsible for Zn transport to the extracellular
529 compartments (Kimura and Kambe, 2016), to restore Zn homeostasis and physiological
530 levels. An increased expression of ZnT-1 transporter and of intracellular zinc levels upon
531 Cd exposure were previously demonstrated by our group in human hepatoma cells (Urani
532 et al., 2010 and 2015). In neurons, a role of ZnT-1 transporter in attenuating cadmium and
533 zinc permeation and toxicity, and the increase of Cd^{2+}-induced neuronal death in ZnT-1
534 siRNA transfected cells was evidenced (Ohana et al., 2006).
535 Very interestingly, strictly linked to Cd effect on Zn transporter discussed above, our results
536 demonstrate that Cd deregulates the expression of genes involved in specific neuronal
537 functions and pathways, giving an overall picture strongly associated to a metal
538 dyshomeostasis and to a damage to neuronal functions and dynamics.
539 Among the top up-regulated genes in our Cd-exposed cells is *HMOX1*, encoding for heme-
540 oxygenase-1 (HO-1). Although beneficial effects of HO-1 as a cytoprotective and anti-
541 inflammatory agent are recognized, an emerging role of increased HO-1 expression in
542 neurodegenerative diseases is evidenced. HO-1 hyperactivity leads to the pathological iron

(Fe) deposition recently observed in various neurodegenerative diseases (Wang et al., 2017, and references therein).

Other Fe-related functions that we found altered in Cd treated SH-SY5Y cells are related to the increased level of *Ferritin*, as highlighted by path views of mineral absorption. In neuronal cells, iron is mostly bound to ferritin or stored in the lysosomes. A variety of neurodegenerative disorders show disturbances in Fe and/or Cu metabolism and excess loading of these metals. The role of Fe, Cu and Zn in the pathophysiology of ALS was previously highlighted. Both animal and *in vitro* models (Lovejoy and Guillemin, 2014), as well as population studies (Qureshi et al., 2008), evidenced elevated ferritin levels in neurodegenerative processes, and a correlation with toxic metal levels (e.g., As, Pb, Hg, Cd) in human samples from ALS patients, suggesting perturbation in iron metabolism by autophagy dysregulation (Biasiotto et al., 2016). In addition, interference of Cd with Fe ions can be mediated by divalent metal transporter 1 protein (DMT1) and transferrin, two Fe^{2+} transporters which can be used by Cd (Kozlowski et al., 2014). Remarkably, as the mechanisms underlying iron absorption are similar to those of Cd, an iron deficiency leads to increased Cd levels, as demonstrated by population studies (see Lee et al., 2014 and references therein).

The interplay and the interference of Cd with other essential metals and ions, are of particular relevance with zinc and calcium, due to their roles in neurotransmission and as signaling elements. Elevation of $[Ca^{2+}]_i$ by Cd in neuronal cells (PC12 and SH-SY5Y), both by extracellular influx and by intracellular release from Ca^{2+} storage, was previously demonstrated and related to neuronal apoptosis (Xu et al., 2011).

One of the 25 top up-regulated genes (*S100A2*) in our cells exposed to cadmium belongs to the highly specialized family of regulatory Ca^{2+}-binding proteins that mediate signal transduction and diseases of the nervous system. Six brain S100 family members, among

568 which S100A2, are hallmarks of normal aging, and they increase in neurodegenerative
569 disorders (Zimmer eta al., 2005). Notably, an increase of S100B, a S100 family member,
570 has been described in neurodegenerative diseases such as Alzheimer's disease,
571 Parkinson's disease and ALS, and new functions as sensors and regulators of zinc levels,
572 as well as a metal-buffering activity of these binding proteins are emerging (Hagmeyer et
573 al., 2018). Moreover, S100A2 is present in the human genome but not in rat/mouse
574 genomes, illustrating the importance of using human models in neurotoxicity studies
575 (Zimmer et al., 2005).
576 Due to the role of glycosphingolipids in neuronal plasma membrane, the dysregulation of
577 this pathway in SH-SY5Y cells suggests possible modifications in neuronal membrane
578 composition and it is tempting to speculate that it may have consequences on recognition of
579 external messenger(s) and their signal transduction pathways (Aureli et al., 2014).
580 Other remarkable altered genes in our cells exposed to cadmium with neuronal-related
581 functions are *NEK3* and *KIF15*. Nek3 protein belongs to a family of Ser-Thr kinases
582 expressed in neurons with critical roles in coordinating microtubule dynamics. In particular,
583 Nek3 was found to have a role in neuronal morphogenesis and polarity through
584 microtubules effects, suggesting that it could be involved in processes related to axonal
585 projections and degeneration (Chang et al., 2009). The Kif15 is a kinesin-related protein, a
586 superfamily of microtubule-based motor proteins with functions ranging from intracellular
587 transport and division. Noteworthy, one member of the kinesin family (KIF5A) was recently
588 identified as a novel gene associated to ALS (Nicolas et al., 2018), strengthening the role of
589 cytoskeletal defects in ALS pathogenesis.
590 The inhibition of microtubule assembly and motility activity of neuronal kinesin were
591 previously demonstrated as consequences of both *in vitro* cadmium exposure and of

elevated non-physiological zinc levels, and is proposed as one molecular cause contributing to neuronal disorders (Böhm, 2014 and 2017).

Other genes that we found among the top up-regulated in SH-SY5Y cells exposed to Cd and relevant for their link to neurodegeneration are *RRAD*, *DDIT3 (*known also as *CHOP)*, and *GDF15*. *RRAD* was recently found up-regulated in the *motor cortex* of sporadic ALS patients, *CHOP* has been linked to the activation of apoptosis signaling in neuroblastoma cells, and GDF15 levels in the cerebrospinal fluid is proposed as a potential marker in disorders such as Parkinson's disease and dementia (Sanfilippo et al., 2017; Soo et al., 2012; Maetzler et al., 2016).

The results of this study on different molecular components and processes altered provide new insights and links on Cd-induced neurotoxicity, and suggest further in depth studies on remedies to counteract the induced essential metal dyshomeostasis.

As concluding remarks, we highlight that toxicogenomics approach is invaluable for mechanistic studies as it provides information on all possible dysregulated genes upon a specific environmental insult. The identification and systematic analysis of up- and down-regulated genes not only provides evidence on functions related to neurodegeneration at a single gene level, but it also gives a comprehensive vision of possible altered processes. In addition, this analysis will help to clarify whether metal-induced cells deregulations are the consequence rather than the cause of neurodegeneration. Deregulated pathways, even not cell-specific, could represent the early triggers for subsequent metabolic and structural unbalances and neurodegeneration.

Finally, the analysis in a controlled environment and standardized neuronal cell model could help in identifying potential biomarkers to be studied in exposed individuals or in the general population.

Conflict of interest statement

There is no potential conflict of interest or competing interest.

Acknowledgements

The Authors acknowledge the University of Milan Bicocca (grant 2016-ATE-0411 to CU and 2017-ATE-0273 to PF) for partial support, and the European Commission. The funding sources had no involvement in data collection, analysis and interpretation, nor in writing and in the decision to submit the article for publication.

REFERENCES

Alhamdoosh M, Ng M, Wilson NJ, Sheridan JM, Huynh H, Wilson MJ, Ritchie ME (2017) Combining multiple tools outperforms individual methods in gene set enrichment analyses. Bioinformatics, 33: 414-424. doi: 10.1093/bioinformatics/btw623

Ardura-Fabregat A, Boddeke EWGM, Boza-Serrano A, Brioschi S, Castro-Gomez S, Ceyzériat K, Dansokho C, Dierkes T, Gelders G, Heneka MT, Hoeijmakers L, Hoffman A, Iaccarino L, Jahnert S, Kuhbandner K, Landreth G, Lonnemann N, Löschmann PA, McManus RM, Paulus A, Reemst K, Sanchez-Caro JM, Tiberi A, Van der Perren A, Vauthney A, Venegas C, Webers A, Weydt P, Wijasa TS, Xiang X, Yang Y (2017) Targeting neuroinflammation to treat Alzheimer's disease. CNS Drugs, 31: 1057-1082. doi: 10.1007/s40263-017-0483-3

ATDSR (2018) Substance Priority List. https://www.atsdr.cdc.gov/spl/resources/index.html (accessed June 10, 2019)

Aude N, Kenna KP, Renton AE, Ticozzi N, et al., (2018) Genome-wide analyses identify KIF5A as a novel ALS gene. Neuron, 97: 1268-1283. doi: 10.1016/j.neuron.2018.02.027

640 Aureli M, Samarani M, Loberto N, Bassi R, Murdica V, Prioni S, Prinetti A, Sonnino S
641 (2014) The glycosphingolipid hydrolases in the central nervous system. Mol Neurobiol
642 50: 76-87. doi: 10.1007/s12035-013-8592-6
643 Babula P, Masarik M, Adam V, Eckschlanger T, Stiborova M, Trnkova L, Skutkova H,
644 Provaznik I, Hubalek J and Kizek R (2012) Mammalian metallothioneins: properties and
645 functions. Metallomics, 4: 739-750. doi: 10.1039/c2mt20081c
646 Barna J, Csermely P, Vellai T (2018) Roles of heat shock factor 1 beyond the heat shock
647 response. Cellular and Molecular Life Sciences 75: 2897-2916. doi: 10.1007/s00018-
648 018-2836-6
649 Bar-Sela S, Reingold S, Richter ED (2001) Amyotrophic lateral sclerosis in a battery-factory
650 worker exposed to cadmium. Int J Occup Environ Health 7: 109-112.
651 doi:10.1179/107735201800339470
652 Biasiotto G, Di Lorenzo D, Archetti S, Zanella I (2016) Iron and neurodegeneration: Is
653 ferritinophagy the link? Mol Neurobiol, 53: 5542-5574. doi: 10.1007/s12035-015-9473-y
654 Bocca B, Pino A, Alimonti A, Forte G (2014) Toxic metals contained in cosmetics: A status
655 report. Reg Toxicol Pharmacol, 68: 447-467. doi: 10.1016/j.yrtph.2014.02.003
656 Böhm KJ (2014) Kinesin-dependent motility generation as target mechanism of cadmium
657 intoxication. Toxicology Letters 224: 356-361. doi: 10.1016/j.toxlet.2013.11.004
658 Böhm KJ (2017) Toxic effects of zinc ions on kinesin – Potential molecular cause of
659 impaired intracellular transport. Toxicology Letters 268: 58-62. doi:
660 10.1016/j.toxlet.2017.01.013
661 Bonham RT, Fine MR, Pollock FM, Shelden EA (2003) Hsp27, Hsp70, and metallothioneins
662 in MDCK and LLC-PK1 renal epithelial cells: effects of prolonged exposure to cadmium.
663 Toxicol Appl Pharmacol 191: 63-73. doi: 10.1016/s0041-008x(03)00226-6

664 Callegaro G, Forcella M, Melchioretto P, Frattini A, Gribaldo L, Fusi P, Fabbri M, Urani C
665 (2018) Toxicogenomics applied to *in vitro* Cell Transformation Assay reveals
666 mechanisms of early response to cadmium. Toxicol in Vitro, 48: 232-243. doi:
667 10.1016/j.tiv.2018.01.025
668 Calvo A, Canosa A, Bertuzzo D, Cugnasco P, Solero L, Clerico M, De Mercanti M, Bersano
669 E, Cammarosano S, Ilardi A, Manera U, Moglia C, Marinou K, Bottacchi E, Pisano F,
670 Mora G, Mazzini L, Chiò A (2016) Influence of cigarette smoking on ALS outcome: a
671 population-based study. J Neurol Neurosurg Psychiatry, 87: 1229-1233. doi:
672 10.1136/jnnp-2016-313793
673 Chang J, Baloh RH, Mildbrandt J (2009) The NIMA-family kinase Nek3 regulates
674 microtubule acetylation in neurons. Journal of Cell Science, 122: 2274-2282. doi:
675 10.1242/jcs.048975
676 Chen QY, DesMarais T, Costa M (2019) Metals and mechanisms of carcinogenesis. Ann
677 Rev Pharmacol Toxicol 59: 537-554. doi: 10.1146/anurev-pharmtox-010818-021031
678 Cheung Y-T, Lau WK-W, Yu M-S, Lai CS-W, Yeung S-C, So K-F, Chang RC-C (2009)
679 Effects of all-*trans*-retinoic acid on human SH-SY5Y neuroblastoma as *in vitro* model in
680 neurotoxicity research. NeuroToxicol, 30: 127-135. doi: 10.1016/j.neuro.2008.11.001
681 Choi S, and Bird AJ (2014) Zinc'ing sensibly: controlling zinc homeostasis at the
682 transcriptional level. Metallomics doi: 10.1039/c4mt00064a
683 Choong G, Liu Y, Templeton DM (2014) Interplay of calcium and cadmium in mediating
684 cadmium toxicity. Chemico-Biol Interac, 211: 54-65. doi: 10.1016/j.cbi.2014.01.007
685 Fabbri M, Urani C, Sacco MG, Procaccianti C, Gribaldo L (2012) Whole genome analysis
686 and microRNAs regulation in HepG2 cells exposed to cadmium. ALTEX, 29: 173-182.
687 doi: 10.14573/altex.2012.2.173

688 Forcella M, Callegaro G, Melchioretto P, Gribaldo L, Frattini M, Stefanini FM, Fusi P, Urani
689 C (2016) Cadmium-transformed cells in the in vitro cell transformation assay reveal
690 different proliferative behaviours and activated pathways. Toxicol in Vitro, 36: 71-80. doi:
691 10.1016/j.tiv.2016.07.006
692 Gokey T, Hang B, Guliaev AB (2016) Cadmium(II) inhibition of human uracil-DNA
693 glycosylase by catalytic water supplantation. Scientific Reports, 6: 39137. doi:
694 10.1038/srep39137
695 Hagmeyer S, Cristòväo JS, Mulvhill JJE, Boeckers T, Gomes CM, Grabrucker AM (2018)
696 Zinc binding to S100B affords regulation of trace metal homeostasis and excitotoxicity in
697 the brain. Front Mol Neurosci 10: 456 doi: 10.3389/fnmol.2017.00456
698 Han SG, Castranova V, Vallyathan V (2007) Comparative cytotoxicity of cadmium and
699 mercury in a human bronchial epithelial cell line (Beas-2B) and its role in oxidative stress
700 and induction of heat shock protein 70. J Toxicol Environ Health A, 70: 852-860. doi:
701 10.1080/15287390701212695
702 Hartwig A (2018) Cadmium and its impact on genomic stability. In “Cadmium interaction
703 with animal cells“ Thévenod et al., Eds., Chapter 5, pagg 107-125. doi: 10.1007/978-3-
704 319-89623-6
705 Hartwig A, and Jahnke G (2017) Toxic metals and metalloids in food. In “Chemical
706 contaminants and residues in food” second edition (Screnk D and Cartus A, Eds.),
707 Chapter 10, pages 209-222. doi: 10.1016/B978-0-08-100674-0.00010-2
708 He G, Xu W, Tong L, Li S, Su S, Tan X, Li C (2016) Gadd45b prevents autophagy and
709 apoptosis against rat cerebral neuron oxygen-glucose deprivation/reperfusion injury.
710 Apoptosis 21: 390-403. doi: 10.1007/s10495-016-1213-x
711 Hung J-J, Cheng T-J, Chang MD-T, Chen K-D, Huang H-L, Lai Y-K (1998) Involvement of
712 heat shock elements and basal transcription elements in the differential induction of the

713 70kDa heat shock protein and its cognate by cadmium chloride in 9L rat brain tumor
714 cells. J Cell Biochem 71: 21-35.
715 Joerger AC and Fersht AR (2016) The p53 pathway: Origins, inactivation in cancer, and
716 emerging therapeutic approaches. Annu. Rev. Biochem, 85: 375-404. 10.1146/annurev-
717 biochem-060815-014710
718 Kalmar B, Lu C-H, Greensmith L (2014) The role of heat shock proteins in Amyotrophic
719 Lateral Sclerosis: The therapeutic potential of Arimoclomol. Pharmacology &
720 Therapeutics, 141: 40-54. doi: 10.1016/j.pharmthera.2013.08.003
721 Karunasinghe N, Masters J, Flanagan JU, Ferguson LR (2017) Influence of aldo-keto
722 reductase 1C3 in prostate cancer – A mini review. Current Cancer Drug Targets, 17:
723 603-616. doi: 10.2174/1568009617666170330115722
724 Kawata K, Kubota S, Eguchi T, Aoyama E, Moritani NH, Oka M, Kawaki H, Tagigawa M
725 (2017) A tumor suppressor gene product, platelet-derived growth factor receptor-like
726 protein controls chondrocyte proliferation and differentiation. Journal of Cellular
727 Biochemistry, 118: 4033-4044. doi: 10.1002/jcb.26059
728 Kimura T and Kambe T (2016) The functions of metallothioneins and ZIP and ZnT
729 transporters: An overview and perspective. International Journal of Molecular Sciences,
730 17: 336-357. doi: 10.3390/ijms17030336
731 Klejnot M, Falnikar A, Ulaganathan V, Cross RA, Baas PW, Kozielski F (2014) The crystal
732 structure and biochemical characterization of Kif15: a bifunctional molecular motor
733 involved in bipolar spindle formation and neuronal development. Acta Crystallographica,
734 D70: 123-133. doi: 10.1107/S1399004713028721
735 Kohli V, Nardini N, Ehrman LA, Waclaw RR (2018) Characterization of Glcci1 expression in
736 a subpopulation of lateral ganglionic eminence progenitors in the mouse telencephalon.
737 Dev Dyn 247: 222-228. doi: 10.1002/dvdy.24556

738 Kostenko S, Jensen KL, Moens U (2014) Phosphorylation of heat shock protein 40
739 (Hsp40/DnaJB1) by mitogen-activated protein kinase-activated protein kinase 5
740 (MK5/PRAK). The International Journal of Biochemistry and Cell Biology, 47: 29-37. doi:
741 10.1016/j.biocel.2013.11.004
742 Kozlowski H, Kolkowska P, Watly J, Krzywoszynska K, Potocki S (2014) General aspects of
743 metal toxicity. Curr Med Chem 21: 3721-3740.
744 Kusakabe T, Nakajima K, Nakazato K, Suzuki S, Takada H, Satoh T, Oikawa M, Arakawa
745 K, Nagamine T (2008) Changes of heavy metal, metallothioneins and heat shock
746 proteins in Sertoli cells induced by cadmium. Toxicol in Vitro 22: 1469-1475. doi:
747 10.1016/j.tiv.2008.04.021
748 Ingre C, Roos PM, Piehl F, Kamel F, Fang F (2015) Risk factors for amyotrophic lateral
749 sclerosis. Clin Epidemiol, 7: 181-193. doi: 10.2147/CLEP.S37505
750 Landry GM, Furrow E, Holmes HL, Hirata T, Kato A, Williams P et al., (2019) Cloning,
751 function, and localization of human, canine, and *Drosophila* ZIP10 (SLC39A10), a Zn^{2+}
752 transporter. Am J Renal Physiol 316: F263-F273. doi: 10.1152/ajprenal.00573.2017
753 Lee B-K, Kim SH, Kim N-S, Ham J-O, Kim Yh (2014) Iron deficiency increases blood
754 cadmium levels in adolescents surveyed in KNHANES 2010-2011. Biol Trace Elem Res,
755 159: 52-58. doi: 10.1007/s12011-014-9982-y
756 Li C, Wang X, Casal I, Wang J, Li P, Zhang W, Xu E, Lai M, Zhang H (2016) Growth
757 differentiation factor 15 is a promising diagnostic and prognostic biomarker in colorectal
758 cancer. Journal Cell and Molecular Medicine, 20: 1420-1426. doi: 10.1111/jcmm.12830
759 Lin J, Chung S, Ueda K, Matsuda K, Nakamura Y, Park J-H (2017) GALNT6 stabilizes
760 GRP78protein by O-glycosylation and enhances its activity to suppress apoptosis under
761 stress condition. Neoplasia, 19: 43-53. doi: 10.1016/j.neo.2016.11.007

762 Liu X-H, Wang Z-J, Jin L, Huang J, Pu D-Y, Wand D-S, Zhang Y-G (2017) Effects of
763 subchronic exposure to waterborne cadmium on H-P-I axis hormones and related genes
764 in rare minnows (*Gobiocypris rarus*). Comparative Biochemistry and Physiology, Part C
765 202: 1-11. doi: 10.1016/j.cbpc.2017.07.002
766 Lovejoy DB and Guillemin GJ (2014) The potential for transition metal-mediated
767 neurodegeneration in amyotrophic lateral sclerosis. Frontiers in Aging Neuroscience, 6
768 article 173, 13 pages doi: 103389/fnagi.2014.00173
769 Luparello C, Sirchia R, Longo A (2011) Cadmium as a transcriptional modulator in human
770 cells. Crit Rev Toxicol 41: 73-80. doi: 10.3109/10408444.2010.529104
771 Maetzler W, Deleersnijder W, Hanssens V, Bernard A, Brockmann K, Marquetand J,
772 Wurster I, Rattay TW, Roncoroni L, Schaeffer E, Lerche S, Apel A, Deuschle C, Berg D
773 (2016) GDF15/MIC1 and MMP9 cerebrospinal fluid levels in Parkinson's disease and
774 Lewy body dementia. PLoS ONE 11(3): e0149349. doi:10.1371/journal.pone.0149349
775 Maret W and Moulis J-M (2013) The bioinorganic chemistry of cadmium in the context of its
776 toxicity. In "Cadmium: From toxicity to essentiality – Metal Ions in Life Sciences" (Sigel A,
777 Sigel H, and Sigel RKO Eds.), Chapter 1, pages 1-29. doi: 10.1007/978-94-007-51798_1
778 Méndez-Armenta M and Rìos C (2007) Cadmium neurotoxicity. Environmental Toxicology
779 and Pharmacology, 23: 350-358. 10.1016/j.etap.2006.11.009
780 Nicolas A, Kenna KP, Renton AE, Ticozzi N, Faghri F, Chia R, Dominov JA, Kenna BJ,
781 Nalls MA, Keagle P, Rivera AM, van Rheenen W, Murphy NA, van Vugt JJFA, Geiger JT,
782 Van der Spek RA, Pliner HA, Shankaracharya, Smith BN, Marangi G, Topp SD,
783 Abramzon Y, Gkazi AS, Eicher JD, Kenna A; ITALSGEN Consortium, Mora G, Calvo A,
784 Mazzini L, et al., (2018) Genome-wide analyses identify KIF5A as a novel ALS gene.
785 Neuron, 97: 1268-1283. doi: 10.1016/j.neuron.2018.02.027

786 Ohana E, Sekler I, Kaisman T, Kahn N, Cove J, Silverman WF, Amsterdam A, Hershfinkel
787 M (2006) Silencing of ZnT-1 expression enhances heavy met influx and toxicity. J Mol
788 Med 84: 753-763. doi: 10.1007/s00109-006-0062-4
789 Pan YB, Zhan CH, Wang SQ, Ai PH, Chen K, Zhu L, Sun ZL, Feng DF (2018) Transforming
790 growth factor beta induced (TGFBI) is a potential signature gene for mesenchymal
791 subtype high-grade glioma. Journal of Neurooncology, 137: 395-407. doi:
792 10.1007/s11060-017-2729-9
793 Park JW, Lee SH, Woo G-H, Kwon H-J, Kim D-Y (2018) Downregulation of TXNIP leads to
794 high proliferative activity and estrogen-dependent cell growth in breast cancer.
795 Biochemical and Biophysical Research Communications, 498: 566-572. doi:
796 10.1016/j.bbrc.2018.03.020
797 Phani S, Jablonski M, Pelta-Heller J, Cai J, Iacovitti L (2013) Gremlin is a novel VTA
798 derived neuroprotective factor for dopamine neurons. Brain Research 1500: 88-98. doi:
799 10.1016/j.brainres.2013.01.017
800 Planells-Palop V, Hazazi A, Feichtinger J, Jezkova J, Thallinger G, Olsiwiheri NO, et al.,
801 (2017) Human germ/stem cell-specific gene *TEX19* influences cancer cell proliferation
802 and cancer prognosis. Molecular Cancer, 16: 84-101. doi: 10.1186/s12943-017-0653-4
803 Prakash A, Bharti K, Bakar A, Majeed ABA (2015) Zinc: indications in brain disorders.
804 Fundamental & Clinical Pharmacology, 29: 131-149. doi: 10.1111/fcp.12110 Qureshi M,
805 Brown Jr RH, Rogers JT, Cudkowicz ME (2008) Serum ferritin and metal levels as risk
806 factors for amyotrophic lateral sclerosis. The Open Neurology Journal, 2: 51-54. doi:
807 10.2174/1874205X00802010051
808 Roos PM, Vesterberg O, Syversen T, Flaten TP, Nordberg M (2013) Metal concentrations
809 in cerebrospinal fluid and blood plasma from patients with amyotrophic lateral sclerosis.
810 Biol Trace Elem Res, 151: 159-170. doi: 10.1007/s12011-012-9547-x

Rossi A, Trotta E, Brandi R, Arisi I, Coccia M, Santoro MG (2010) *AIRAP,* a new human heat shock gene regulated by heat shock factor 1. Journal of Biological Chemistry, 285: 13607-13615. doi: 10.1074/jbc.M109.082693

Rossi S, Serrano A, Gerbino V, Giorgi A, Di Francesco L, Nencini M, Bozzo F, Schininà ME, Bagni C, Cestra G, Carrì MT, Achsel T, Cozzolino M (2015) Nuclear accumulation of mRNAs underlies G4C2-repeat-induced translational repression in a cellular model of *C9orf72* ALS. J Cell Sci, 128: 1787-1799. doi: 10.1242/jcs.165332

Sanfilippo C, Longo A, Lazzara F, Cambria D, Distefano G, Palumbo M, Cantarella A, Malaguarnera I, Di Rosa M (2017) *Chi3L1* and *CHI3L2* overexpression in motor cortex and spinal cord of sALS patients. Molecular and Cellular Neuroscience 85: 162-169. doi: 10.1016/j.mcn.2017.10.001

Sarchielli E, Pacini S, Morussi G, Punzi T, Marini M, Vannelli GB, Gulisano M (2012) Cadmium induces alterations in the human spinal cord morphogenesis. Biometals 25: 63-74. doi: 10.1007/s10534-011-9483-9

Satarung S and Moore MR (2004) Adverse health effects of chronic exposure to low-level cadmium in foodstuff and cigarette smoke. Environ Health Persp 112: 1099-1103. doi: 10.1289/ehp.6751

Sheykhansari S, Kozielski K, Bill J, Sitti M, Gemmati D, Zamboni P and Singh AV (2018) Redox metals homeostasis in multiple sclerosis and amyotrophic lateral sclerosis: a review. Cell Death & Disease 9: 348-363. doi: 10.1038/s41419-018-0379-2

Smyth, GK. (2004) Linear models and empirical bayes methods for assessing differential expression in microarray experiments. Stat Appl Genet Mol Biol 3, Article3. doi:10.2202/1544-6115.1027

834 Soo KY, Atkin JD, Farg M, Walker AK, Horne MK, Nagley P (2012) Bim links ER stress and
835 apoptosis in cells expressing mutant SOD1 associate with amyotrophic lateral sclerosis.
836 PLoS ONE 7(4): e35413. doi: 10.1371/journal.pone.0035413
837 Syk-Mazurek SB, SB, Fernandes KA, Wilson MP, Shrager P, and Libby RT (2017)
838 Together JUN and DDIT3 (CHOP) control retinal ganglion cell death after axonal injury.
839 Molecular Neurodegeneration, 12: 71-84. doi: 10.1186/s13024-017-0214-8
840 Urani C, Melchioretto P, Gribaldo L (2010) Regulation of metallothioneins and ZnT-1
841 transporter expression in human hepatoma cells HepG2 exposed to zinc and cadmium.
842 Toxicol In Vitro, 24: 370-374. doi: 10.1016/j.tiv.2009.11.003
843 Urani C, Melchioretto P, Canevali C, Morazzoni F, Gribaldo L (2007) Metallothionein and
844 hsp70 expression in HepG2 cells after prolonged cadmium exposure. Toxicol. In Vitro
845 21: 314-319. doi: 10.1016/j.tiv.2006.08.014
846 Urani C, Melchioretto P, Bruschi M, Fabbri M, Sacco MG, Gribaldo L (2015) Impact of
847 Cadmium on Intracellular Zinc Levels in HepG2 Cells: Quantitative Evaluations and
848 Molecular Effects. Biomed Res Int, article ID 949514, pages 1-11. doi:
849 10.1155/2015/949514
850 Wang B and Du Y (2013) Cadmium and its neurotoxic effects. Oxidative Medicine and
851 Cellular Longevity, Article ID 898034, 12 pp. doi: 10.1155/2013/898034
852 Wang M-D, Little J, Gomes J, Cashman NR, Krewski D (2017) Identification of risk factors
853 associated with onset and progression of amyotrophic lateral sclerosis using systematic
854 review and meta-analysis. NeuroToxicol, 61: 101-130. doi: 10.1016/j.neuro.2016.06.015
855 Xu B, Chen S, Luo Y, Chen Z, Liu L, Zhou H, Chen W, Han X, Chen L, Huang S (2011)
856 Calcium signaling is involved in cadmium-induced neuronal apoptosis via induction of
857 reactive oxygen species and activation of MAPK/mTOR network. PLoS ONE 64: e19052
858 doi: 10.1371/journal.pone.0019052.

Yeom S-Y, Nam D-H, Park C (2014) RRAD promotes EGFR-mediated STAT3 activation and induces Temozolomide resistance of malignant glioblastoma. Molecular Cancer Therapeutics, 13: 3049-3061. doi: 10.1158/1535-7163.MCT-14-0244

Zhang Z, Hao C-J, Li C-G, Zang D-J, Zhao J, Li X-N, Wei A-H, Wei Z-B, Yang L, Zhen X-C, Gao X, Speakman JR, Li W (2014) Mutation of SLC35D causes metabolic syndrome by impairing dopamine signaling in striatal D1 neurons. PLOS Genetics 10: e1004124. doi: 10.1371/journal.pgen.1004124

Zimmer DB, Chaplin J, Baldwin A, Rast M (2005) S100-mediated signal transduction in the nervous system and neurological diseases. Cellular and Molecular Biology, 51: 201-214.

Figure

Click here to download high resolution image

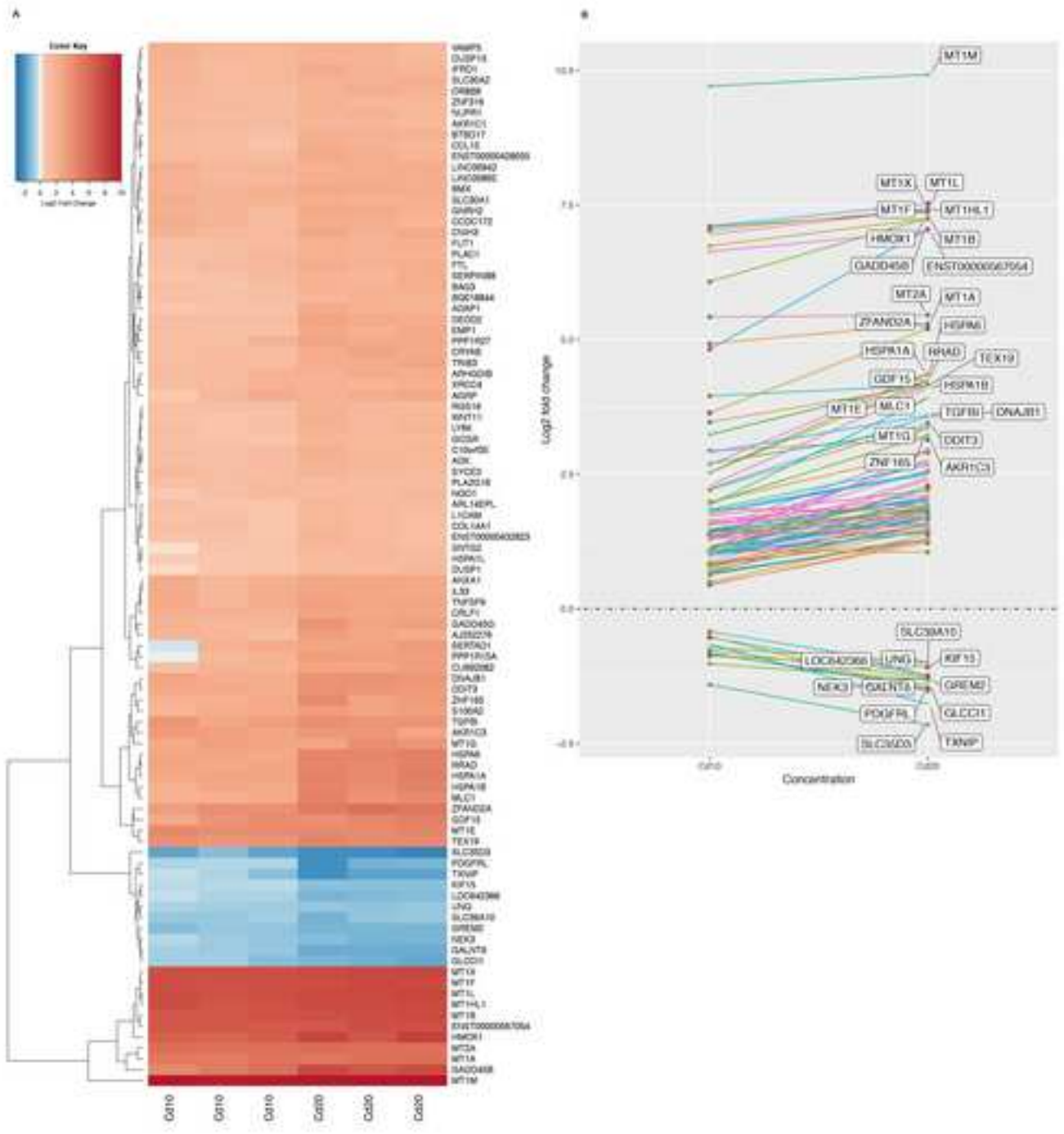

Figure

Click here to download high resolution image

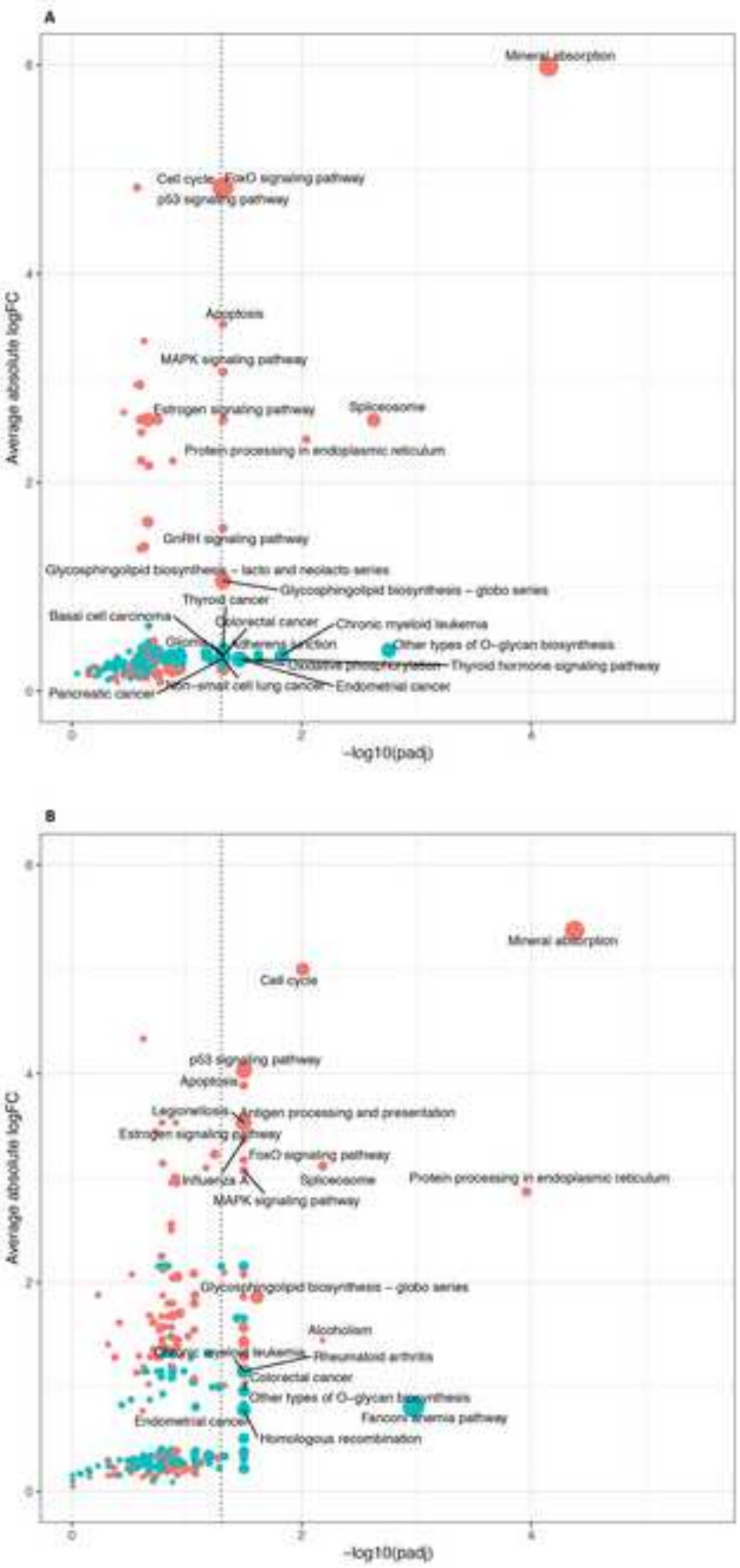

Figure

Click here to download high resolution image

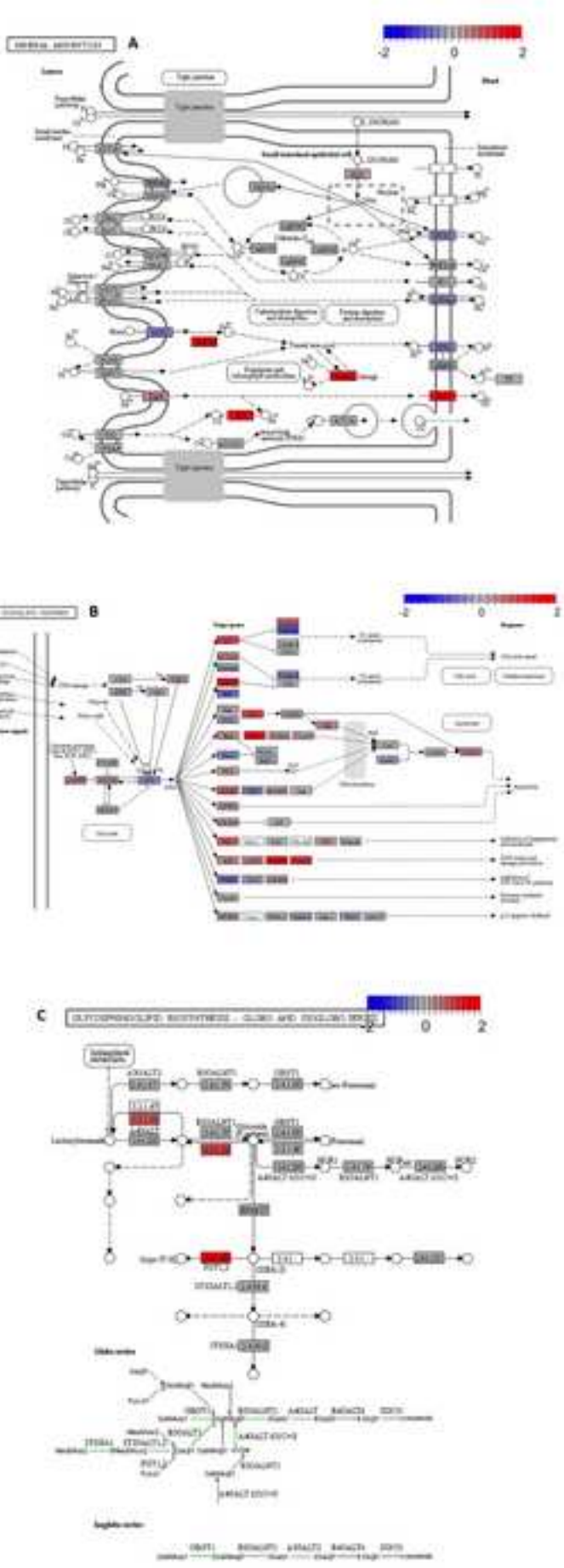

Figure
Click here to download high resolution image

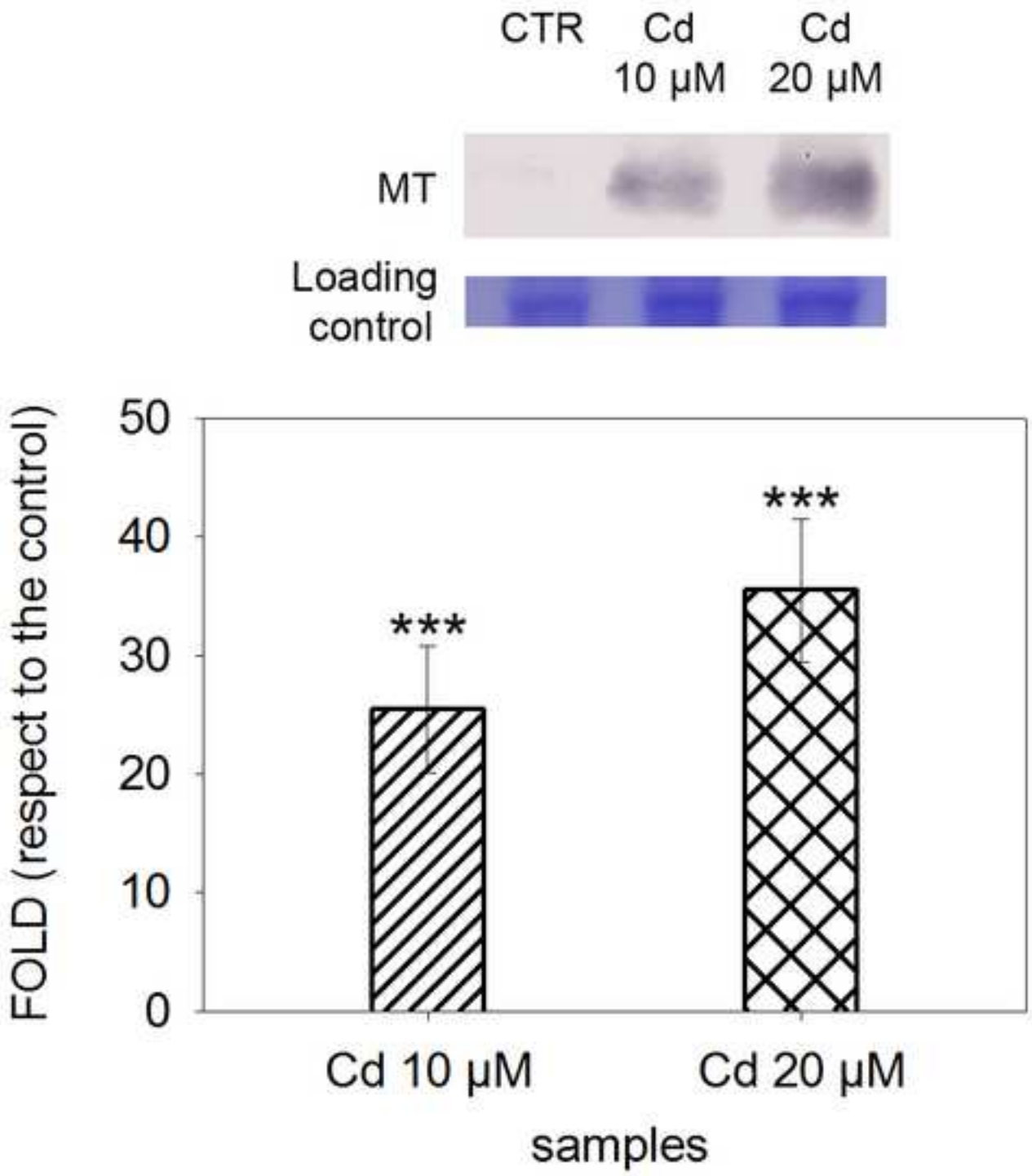

Figure
Click here to download high resolution image

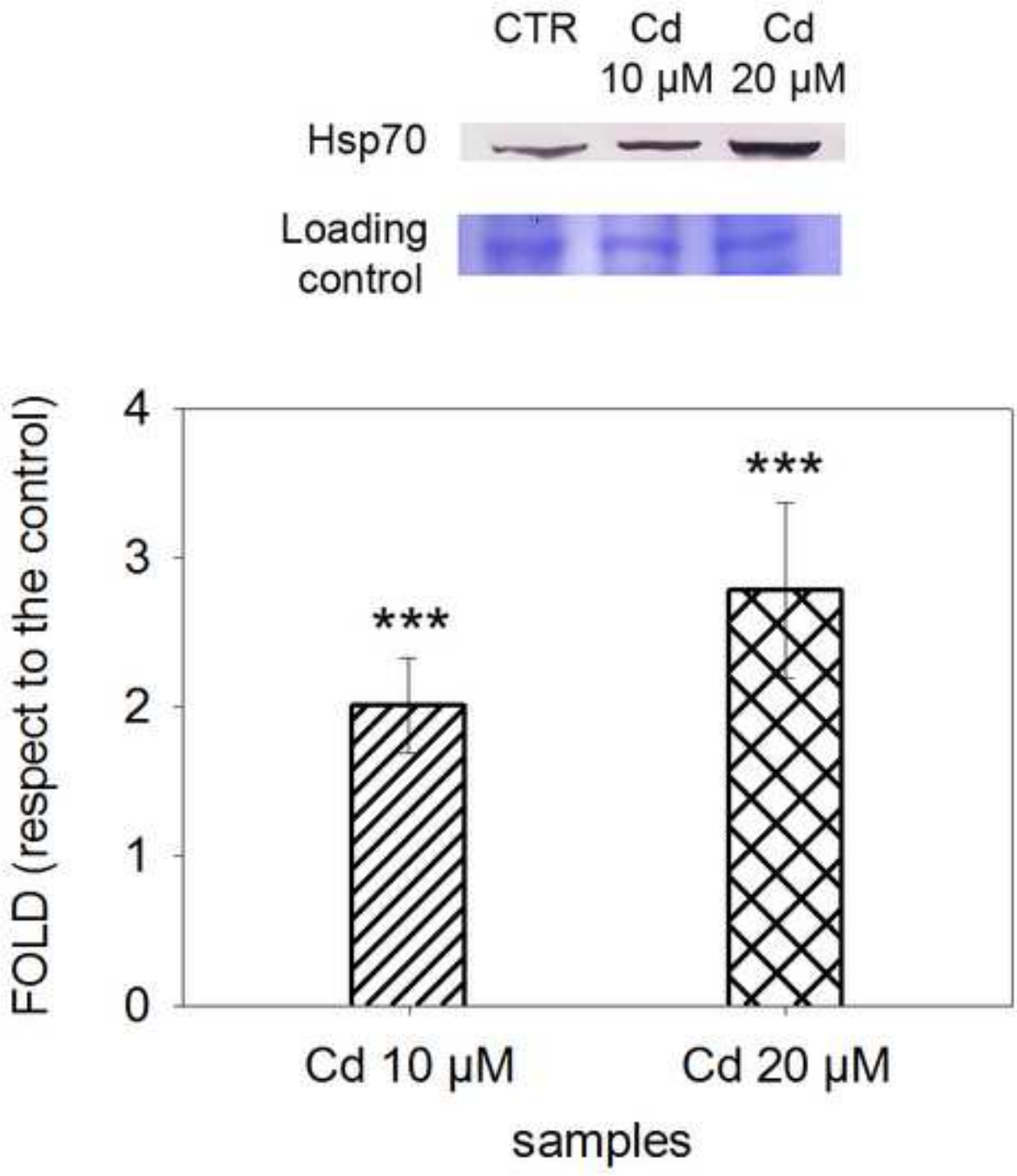

Figure

Click here to download high resolution image

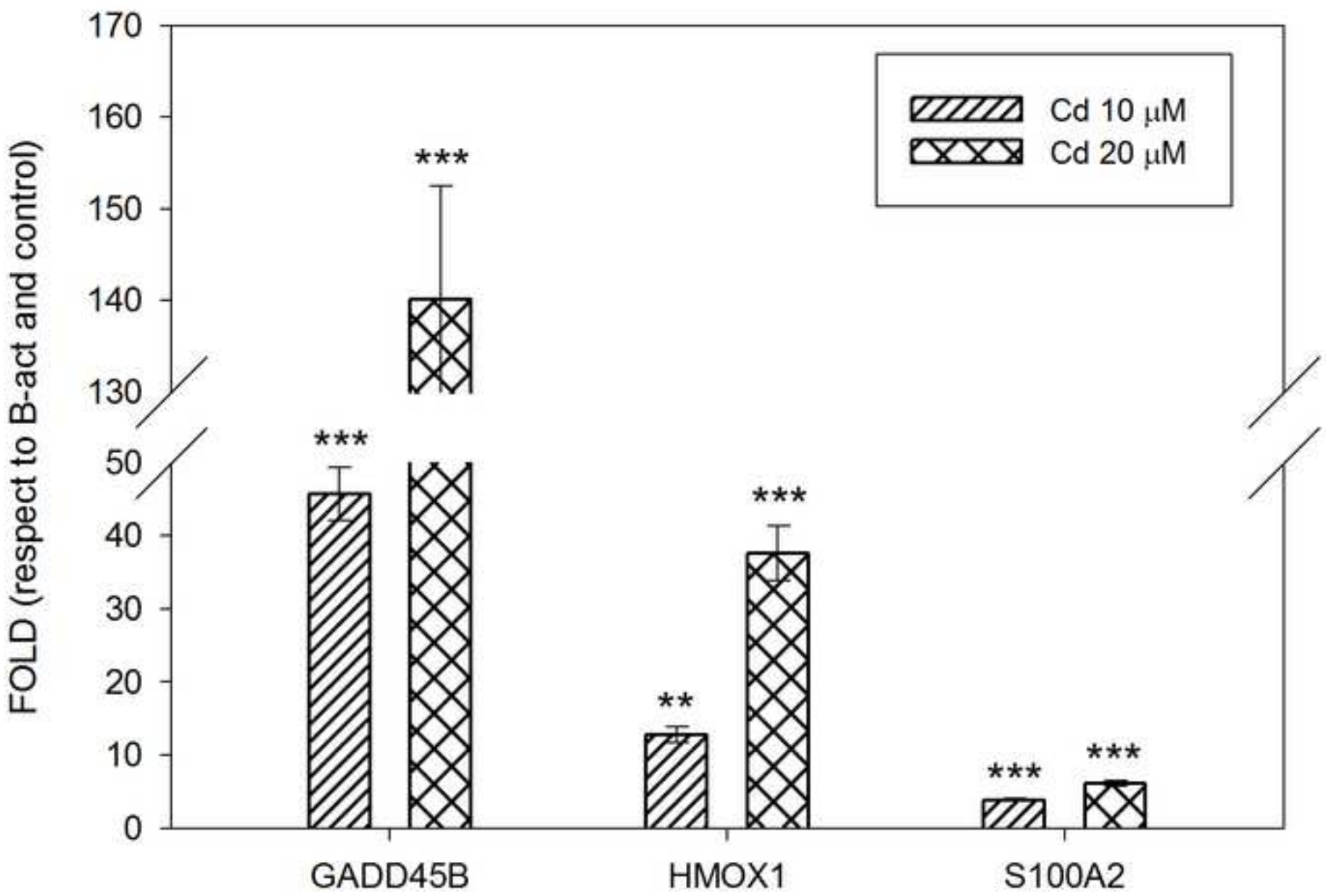

Table 1

Top up-regulated genes in SH-SY5Y cells treated with 10 or 20 μM Cd for 48 h

Gene	Cd10 μM log fold change	Cd20 μM log fold change	adj.P.Value	Description
MT1M	9,71	9,92	2,61E-05	metallothionein 1M
MT1X	7,11	7,53	7,53E-05	metallothionein 1X
MT1F	7,10	7,37	8,98E-05	metallothionein 1F
MT1L	7,04	7,43	3,84E-05	metallothionein 1L (gene/pseudogene)
MT1HL1	6,95	7,42	3,84E-05	Metallothionein 1H-like protein 1
MT1B	6,74	7,25	2,61E-05	metallothionein 1B
ENST00000567054	6,63	7,02	3,84E-05	NA
HMOX1	6,08	7,26	0,001731748	heme oxygenase (decycling) 1
MT2A	5,42	5,45	0,000160204	metallothionein 2A
MT1A	4,92	5,29	0,00014948	metallothionein 1A
GADD45β	4,82	7,05	0,000545108	growth arrest and DNA-damage-inducible, beta
MT1E	3,95	4,15	0,000250941	metallothionein 1E
ZFAND2A	3,64	5,20	0,006524353	zinc finger, AN1-type domain 2A
TEX19	3,47	4,15	0,003753672	testis expressed 19
GDF15	3,24	4,22	0,002993824	growth differentiation factor 15
AKR1C3	2,94	3,14	0,002993824	aldo-keto reductase family 1, member C3 (3-alpha hydroxysteroid dehydrogenase, type II)
TGFBI	2,90	3,59	0,013115332	transforming growth factor, beta-induced, 68kDa
MT1G	2,70	3,36	0,034682665	metallothionein 1G
HSPA1A	2,67	4,38	0,005651168	heat shock 70kDa protein 1A
HSPA6	2,53	4,36	0,000545108	heat shock 70kDa protein 6 (HSP70B')
RRAD	2,53	4,24	0,00208082	Ras-related associated with diabetes
HSPA1B	2,29	4,10	0,014428639	heat shock 70kDa protein 1B
DNAJB1	2,23	3,57	0,001731748	DnaJ (Hsp40) homolog, subfamily B, member 1
DDIT3	2,21	3,45	0,000545108	DNA-damage-inducible transcript 3
S100A2	1,98	2,91	0,001731748	S100 calcium binding protein A2

Table 2

Complete list of down-regulated genes in SH-SY5Y cells treated with 10 or 20 μM Cd for 48 h

Gene	Cd10 μM log fold change	Cd20 μM log fold change	adj.P.Value	Description
SLC35D3	-1,41	-2,15	0,03018534	solute carrier family 35, member D3
GREM2	-1,02	-1,32	0,02198818	gremlin 2
SLC39A10	-0,88	-1,07	0,04704006	solute carrier family 39 (zinc transporter), member 10
GLCCI1	-0,84	-1,42	0,02971039	glucocorticoid induced transcript 1
GALNT6	-0,82	-1,48	0,03741771	UDP-N-acetyl-alpha-D-galactosamine:polypeptide N-acetylgalactosaminyltransferase 6 (GalNAc-T6)
NEK3	-0,77	-1,28	0,04518064	NIMA (never in mitosis gene a)-related kinase 3
UNG	-0,72	-1,00	0,04826738	uracil-DNA glycosylase
TXNIP	-0,65	-1,77	0,01403976	thioredoxin interacting protein
LOC642366	-0,53	-1,24	0,04997033	uncharacterized LOC642366
PDGFRL	-0,51	-1,53	0,02586179	platelet-derived growth factor receptor-like
KIF15	-0,42	-1,09	0,03768701	kinesin family member 15

Supplementary Material

Click here to download Supplementary Material: Table 1S.xlsx

Supplementary Material

Click here to download Supplementary Material: Table 2S.xlsx

Supplementary Material

Click here to download Supplementary Material: Table 3S.xlsx

Supplementary Material

Click here to download Supplementary Material: Figure 1S.jpg

Supplementary Material

Click here to download Supplementary Material: Figure 2S.jpg